REPORT DOCUMENTATION PAGE

AFRL-SR-BL-TR-99-

0220

1. AGENCY USE ONLY (Leave blank)	2. REPORT DATE	3. REPOF
		01 May 96 to 30 Apr 99 Final

4. TITLE AND SUBTITLE
(JSEP) Ultra-high speed compound Semiconductor Photonics

5. FUNDING NUMBERS
61102F
2305/AX, FX and EX

6. AUTHOR(S)
Professor Krusius

7. PERFORMING ORGANIZATION NAME(S) AND ADDRESS(ES)
Cornell University
120 Day Hall
Ithaca NY 14853-2801

8. PERFORMING ORGANIZATION REPORT NUMBER

9. SPONSORING/MONITORING AGENCY NAME(S) AND ADDRESS(ES)
AFOSR/NE
801 North Randolph Street Rm 732
Arlington, VA 22203-1977

10. SPONSORING/MONITORING AGENCY REPORT NUMBER

F49620-961-0162

11. SUPPLEMENTARY NOTES

12a. DISTRIBUTION AVAILABILITY STATEMENT
APPROVAL FOR PUBLIC RELEASED; DISTRIBUTION UNLIMITED

12b. DISTRIBUTION CODE

13. ABSTRACT *(Maximum 200 words)*

Significant growth stimulation by laser irradiation during the OMVPE process is only possible in the kinetically limited regime, which is traditionally avoided. We thus carried out a detailed study on the material properties of low temperature grown AlGaAs and on the reaction mechanisms involved in its synthesis. Growth conditions were similar to those employed during the excimer laser stimulation experiments.

14. SUBJECT TERMS

15. NUMBER OF PAGES

16. PRICE CODE

17. SECURITY CLASSIFICATION OF REPORT	18. SECURITY CLASSIFICATION OF THIS PAGE	19. SECURITY CLASSIFICATION OF ABSTRACT	20. LIMITATION OF ABSTRACT
UNCLASSIFIED	UNCLASSIFIED	UNCLASSIFIED	UL

19990915060

Final Report

**Ultra-High Speed Compound
Semiconductor Photonics**

May 1, 1996 – April 30, 1999

Contract #F49620-96-C-0162

**J.P. Krusius
Principal Investigator**

**Cornell University
School for Electrical Engineering
Ithaca, New York 14853**

Table of Contents

Overview

This document is the final technical report of the Cornell Joint Services Electronics Program for the period from May 1, 1996 to April 30, 1999. The program has been in phase-out over most of this period following the nationwide termination of JSEP. Only during the first year the program was funded at the level of the three-year program that was to start on May 1, 1996. Funding was steadily decreased during the second and third years. This program has covered compound semiconductors materials growth, femtosecond optical sources and characterization of materials and devices, device physics and simulation, device design and fabrication components in a synergistic fashion. Six task investigators, Profs. R. Shealy, C. Tang, C. Pollock, P. Krusius, Y. Lo and R. Compton, with their graduate students have contributed to this JSEP research. Research interactions and collaborations between the participating groups have continued, although their impact has been much less significant with task investigators exploring other funding opportunities for their research.

The Cornell JSEP faculty has long traditions in compound semiconductor materials, electronic devices, femtosecond optical sources and measurements methods, photonic devices, micro- and nanofabrication and device physics. Indicators of this strength are, for example: past JSEP programs, which during their 16 year history have focused on compound semiconductor materials and high speed electronic devices and femtosecond optics; the Optoelectronics Technology Center, a consortium formed by Cornell University, University of California Santa Barbara, University of California San Diego, and supported by DARPA; the Cornell Nanofabrication Facility supported by the National Science Foundation and industry, which has been continually funded since 1977 and now is one of the major nodes in the National Nanofabrication Network; the Materials Science Center supported by the National Science Foundation; the Cornell Center for Theory and Simulation, one of the national supercomputer centers supported by the National Science Foundation; and many individual programs supported by federal and industrial sources. Other Cornell facilities relevant to this program include the unique Compound Semiconductor Materials Growth Facility with several OMVPE reactors; the Optoelectronics Laboratory for optical experiments and measurements within the School of Electrical Engineering; and several unique tunable femtosecond laser based optical characterization laboratories.

As a consequence of the phaseout the total funding for the three year program was reduced by 22% compared to the original plan. The resources among the tasks were shifted as well to reflect the level of effort and different responses to the phaseout. Resources were shifted out from tasks #4 (Krusius) and task #5 (Compton) into tasks #1 (Shealy), task #2 (Tang), and task #5 (Lo) compared to the original plan. These shifts impacted activity levels and hence results as well.

Specific results obtained in the individual work units are given separately in the sections covering each task and will not be repeated here. 1 Master of Science degrees, 5 Master of Engineering, and 8 PhD degrees have been granted to students working on these JSEP tasks during the 1996/99 program period. At the same time 56 publications have published, submitted, or are in preparation for to scientific or technical periodicals and 28 related publications have been prepared.

2. Principal Investigators

Principal Investigator/Task	Task Title
James R. Shealy/Task #1	OMVPE Growth of III-V Alloys for New High Speed Electron Devices
C.L. Tang/Task #2	Broadly Tunable Femtosecond Sources and Ultrafast Properties of Optical Materials
C. R. Pollock/Task #3	Controlling Chaos in Lasers and Femtosecond Characterization of Semiconductor Devices
J.P. Krusius/Task #4	Laser Physics for Long Wavelength High Speed Applications
Y.H. Lo/Task #5	Long Wavelength Vertical Cavity Lasers for High Speed Communication
R. Compton/W.Wright/Task #6	Schottky Formation on GaInP/ GaInAs and AlInP/GaInAs for Use in Long Wavelength Detectors and High Power HEMT's

TASK #1 OMVPE GROWTH Of III-V ALLOYS FOR NEW HIGH SPEED ELECTRON DEVICES

Principal Investigator : James R. Shealy, (607) 255-4657

OBJECTIVE

In our effort to understand the fundamentals of UV laser stimulated OMVPE and to develop it as a technique for high-resolution in-situ area-selective deposition of thin films, we investigated the stimulation mechanisms and characteristics of the growth enhancement around 250 nm using an excimer-pumped dye laser system as well as a frequency doubled Ar^+ ion laser. In support, a detailed study of the material properties of AlGaAs grown in the kinetically limited regime was carried out. Finally, we succeeded in the laser stimulated selective-area growth of quantum dots.

DISCUSSION OF STATE-OF-THE-ART

UV-stimulated GaAs growth by MOMBE [1-3], CBE [4] and OMVPE [5-10] has been demonstrated over a wide range of experimental conditions using pulsed laser sources or UV-lamps. Many of these studies have shown significant growth rate enhancements in the irradiated areas. UV irradiation during low temperature growth has also been shown to improve the crystalline quality of the grown layers [3,5]. To our knowledge, there are no reports to this date on CW laser stimulated growth around 250nm wavelength, the regime where both our excimer laser and CW laser experiments were conducted.

PROGRESS

Significant growth stimulation by laser irradiation during the OMVPE process is only possible in the kinetically limited regime, which is traditionally avoided. We thus carried out a detailed study on the material properties of low temperature grown AlGaAs and on the reaction mechanisms involved in its synthesis. Growth conditions were similar to those employed during the excimer laser stimulation experiments.

AlGaAs grown from methyl precursors at low temperatures is known to exhibit high unintentional carbon doping with significant hydrogen passivation of the carbon acceptors. Carbon from the methyl ligands of the organometallic precursors is incorporated via a secondary growth mechanism involving the formation of carbene [11]. Since this pathway competes with the dominant reaction between organometallics and hydrides, increasing carbon doping is expected for lower V/III ratios with carbon substituting arsenic in the crystal lattice. Both, this dependence on V/III ratio and the p-type behavior were confirmed. Since the tetrahedral covalent bond radius of carbon is much smaller than that of gallium, aluminum or arsenic, high carbon concentrations in AlGaAs lead to significant lattice contraction. Since it is not possible to determine the composition of heavily carbon doped AlGaAs from its lattice constant, we measured composition independently by Rutherford backscattering. Figure 1(a) shows the Al mole fraction in the solid as function of V/III ratio, where the upper curve corresponds to 75% trimethylaluminum (TMA) in the total group III flux, and the lower curve to 45%. The overall growth rate under these experimental conditions is strongly limited by the amount of arsine supplied. The decreasing Al solid mole fraction with decreasing V/III ratio at higher arsine flows suggests that the surface reaction of trimethylgallium (TMG) is favored over that of TMA in the competition for arsine. The most interesting aspect about the compositional dependence on V/III ratio, however, is its anomalous behavior around unity V/III ratio. The fact that the Al incorporation into the layer is not a monotonous function of the amount of arsine supplied must be due to either a drastic shift between the rates of the different reactions and/or the relevance of a new reaction pathway at low V/III ratios. The only confirming data of this anomalous behavior found in

the literature results from the decomposition experiments by Mashita [12]. His study was also carried out in a vertical flow system at low pressure. Figure 1(b) reproduces Mashita's data for the decomposition of TMA at
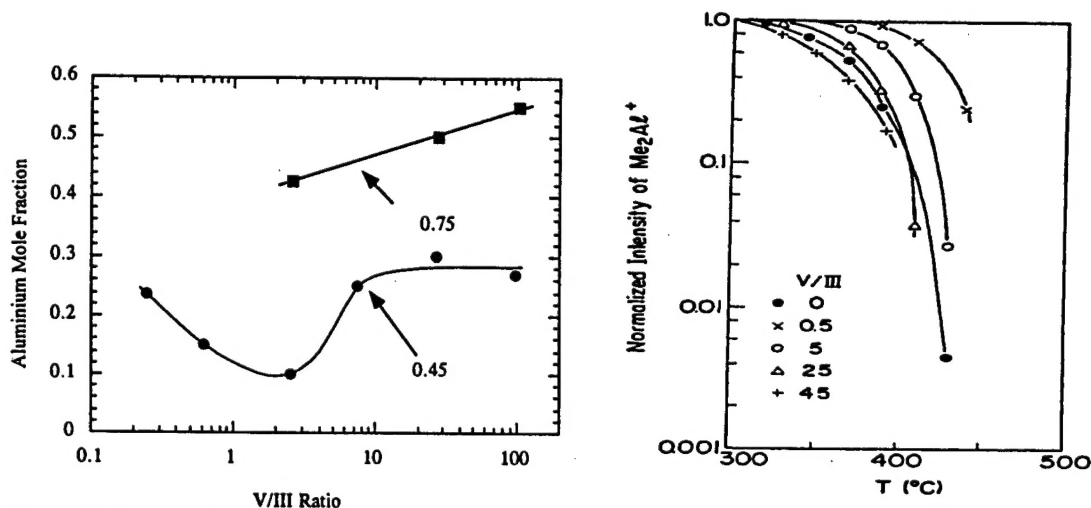
Figure 1(a). Al mole fraction measured by RBS as a function of V/III ratio.

Figure 1(b). Dependence of Me_2Al^+ intensity generated from TMA on temperature.

different V/III ratios. It shows the Me_2Al^+ intensity as detected downstream by a quadrupole mass spectrometer and normalized to the initial intensity. The addition of a small amount of arsine suppresses TMA decomposition, whereas it is enhanced at higher V/III ratios. This contrasts the gradual enhancement of TMG decomposition with increasing arsine partial pressures [12]. The most likely explanation for this phenomenon is the formation of a more stable adduct between the TMA dimer and arsine. Further reaction of the adduct with arsine, either homogeneously or heterogeneously, results then in the increasing decomposition at higher V/III ratios. The correspondence to our compositional data shows the immediate relevance of this peculiarity in TMA chemistry to AlGaAs growth in the kinetically limited regime. The effect on layer composition is further enhanced by the different decomposition behavior of TMG and the resulting shift between the AlAs and GaAs reaction rates.

The most interesting effect of the high unintentional carbon doping with respect to material properties was observed to be on the optical characteristics of the AlGaAs layers. Focusing on the samples grown at 45% aluminum vapor mole fraction, the steady increase in carbon concentration as the V/III ratio was lowered resulted in significant shifts of the photoluminescence peaks. Since the aluminum mole fraction in the layer varies with V/III ratio, we consider for each sample the difference between the actual peak position and the nominal bandgap at the respective temperature. Thus we obtain with $(h\nu-E_g)$ a quantity independent of the composition and sample temperature. Two each other opposing effects influence the bandgap of our highly carbon doped AlGaAs layers: bandtail states introduced by the degenerate doping shrink the bandgap, and the compressive strain due to the smaller carbon atoms widens the bandgap. Considering the bandgap as a function of V/III ratio, we establish, that the effect of compressive strain dominates the bandtail effect, if the slope of $(h\nu-E_g)$ as function of V/III ratio is negative. Conversely, if the slope is positive, the bandtail effect dominates the effect of compressive strain. Figure 2(a) shows the dependence of $(h\nu-E_g)$ on V/III ratio for the room temperature luminescence spectra of as-grown (open circles) and annealed (solid circles) samples, and figure 2(b) shows the corresponding for low temperature photoluminescence. The curves are drawn qualitatively as a guide to the eye and the division into three regions is also qualitative in nature. The dependencies of $(h\nu-E_g)$ on V/III ratio agree well for room and low temperature
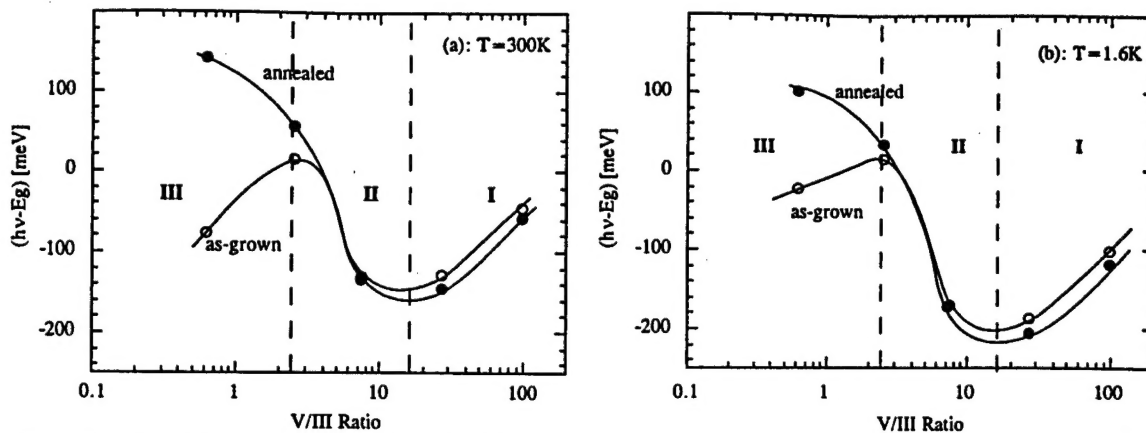
6

Figure 2. (hv-E_g) vs. V/III ratio for (a) 300K and (b) 1.6K photoluminescence spectra of the samples grown at 0.45 aluminum vapor mole fraction. The two curves correspond to annealed and as-grown samples as indicated.

photoluminescence spectra. From our previous discussion we conclude, that the bandtail states affect the bandgap more than compressive strain in region I, and that the strain dominates in region II. For the low V/III ratios in region III we observe a transition from bandtail effect to compressive strain effect dominance upon annealing. At these high carbon concentrations, the gain in free carriers through the anneal affects the bandgap so much more than the additional lattice contraction due to the hydrogen purge, that this transition occurs. Overall, we can conclude that the two opposing effects on the bandgap are equally important in heavily carbon doped AlGaAs.

Our study on deep-UV excimer laser stimulated growth of AlGaAs, which we reported previously in more detail, yielded the following major results. A significant growth contrast (growth in light : growth in dark) of 3.2 : 1 was obtained under the employed experimental conditions. The laser spot surface exhibited over large regions a homogeneous periodic ripple structure, which arises from an intensity modulation of the electromagnetic intensity at the surface, caused by the interference between the incident laser beam and a surface propagating plasma wave [13]. Varying the excitation wavelength continuously from 235nm to 255nm, we found an abrupt drop to zero enhanced growth for wavelengths greater than 252nm. Through simulation of the laser-induced surface temperature rise, we could exclude laser-induced local heating as the dominant stimulation mechanism. Furthermore, since the ripple formation is a surface phenomenon, gas phase photolysis can not be responsible for the growth enhancement under illumination. The measured wavelength edge, at photon energies much higher than the bandgap, further excludes reaction catalysis through carrier generation near the semiconductor surface. This only leaves photolysis of the chemisorbed adlayer as the dominant stimulation mechanism, which is consistent with the abruptness of the wavelength edge indicating a quantum transition. With the knowledge gained about growth mechanisms during low temperature AlGaAs growth and about the effect of the high unintentional carbon doping on the material properties, we could conclude that the growth enhancement results from an acceleration rather than a drastic alteration of the growth reactions.

Due to the unsatisfactory beam quality of the excimer laser for high resolution optical patterning and the difficulty to control the optical power, we switched to a frequency doubled Ar+ laser with output at 248nm and 257nm wavelength. Investigating growth stimulation of different materials from a variety of precursors, we succeeded in the laser enhanced growth of GaAs, InAs and InP from the organometallics trimethylgallium, triethylgallium and trimethylindium and the hydrides arsine and phosphine. Significant growth stimulation of all these materials was obtained at 248nm as well as 257nm. Since the cut-off wavelength of 252nm for growth enhancement under excimer laser illumination falls between these two available wavelengths, the dominant stimulation mechanism with a CW laser source must differ from that in the previous study. Depending on both laser and growth parameters, smooth growth surfaces or the formation of periodic surface ripples were observed in the stimulated growth region. Since the laser-induced temperature rise due to the CW laser is even less significant than in the excimer laser case, reaction catalysis through photo-generated carriers constitutes the dominant CW laser stimulation mechanism.

The formation of the laser induced surface ripples, which we observed the first time for CW laser stimulated semiconductor growth, along with the possibility to accurately control the beam intensity caused us to investigate this phenomenon in further detail. According to the widely accepted theory by Sipe et al. [13], the patterns result from inhomogeneous energy absorption just beneath the surface, originally induced by surface roughness. The interference between the incident laser beam and the laser-induced surface propagating electromagnetic wave results in a standing wave pattern, which in turn leads to periodic variations in the intensity of the electromagnetic radiation at the surface. Our results agree with the predicted laser polarization dependence of direction and periodicity of these gratings. The periodicity is a function of wavelength and angle of incidence. The dynamic evolution of these structures is believed to strongly depend on a positive feedback mechanism [14]. The surface modification results from the growth enhancement response to the intensity modulation and, in turn, enforces the standing wave amplitude. Barborica et al. [15] investigated this system theoretically based on a simple linear surface response model. Their simulations in form of a dynamic system with nonlinear delayed feedback predicts stable regions, where the periodic structure is maintained, as well as random surface structures arising through the subharmonic way to chaos. For the semiconductor melting by excimer lasers they investigated, the chaotic regime occurs at higher laser powers. Figure 3 on the next page shows a collection of atomic force microscopy images taken at the center of GaAs laser-stimulated spots grown under different conditions. Laser intensity and growth temperature were varied in the two-dimensional array fashion indicated. All samples were grown from triethylgallium and arsine for two minutes. The surface morphology varies under these experimental conditions from smooth growth over pronounced homogenous surface ripples to random island formation. In accordance with the positive feedback model, we observe a chaotic regime at high laser intensities coupled with low growth temperatures. The growth contrast varies in dependence on the feedback from 3 : 1 (smooth) to 135 : 1 (chaotic). These experiments show that the degree of feedback is equally dependent on laser intensity and growth temperature. The latter is the key parameter to the reaction kinetics and thus growth rate. Since increased feedback is observed at lower growth temperatures, we believe the increased dark growth rate at higher temperatures to be responsible for the suppression of positive feedback. Under the right set of conditions, long range ordered homogeneous submicron gratings can be produced in-situ for potential application in optical devices.

Selective area growth with sub-micron patterning resolution could offer the desired additional control over InAs island formation via the Stranski-Krastanov growth mode. Thus, we investigated the selective area growth of InAs quantum dots (QDs) by UV photostimulation. The growth was conducted at 435°C on a GaAs substrate with a 3000Å GaAs buffer. InAs from trimethylindium and arsine was deposited with exposure to the 248nm laser beam for 0.75 seconds and, after an 8 second growth stop, capped with 150Å GaAs. The laser beam was focused onto the sample to a spot size of ~ 0.8 mm (FWHM), resulting in a power density of 43W/cm^2. Laser stimulated growth of bulk InAs under these conditions showed a 30% growth enhancement.

Figure 4 compares a 77K unpolarized photoluminescence spectrum taken in the dark grown region (Fig. 4a) to the spectrum from the center of the UV laser stimulated growth spot (Fig. 4b). The spectra were recorded subsequently under identical conditions and are displayed on the same intensity scale. A probing laser spot size of about 300µm diameter (FWHM) at 10W/cm^2 was used. The UV laser excited growth region exhibits both QD and wetting layer (WL) luminescence at 1.358 eV and 1.435 eV respectively, whereas only the WL peak at 1.445 eV is present in the unstimulated region. Thus, the 30% InAs growth rate enhancement causes the transition from 2D to 3D growth mode to occur in the laser stimulated region only. The QD transition energy is in good agreement with theoretical predictions [16] for our measured island size of 7-9 nm diameter, and spectra comparable to that in figure 4 (b) can be found in the literature [17].

Laser / Growth	Spot Diameter 100 μm	Spot Diameter 150 μm	Spot Diameter 200 μm
Growth Temperature 350°C Growth Rate in the Dark 0.21 μm/ hr	z_{max}: 300 nm Center	z_{max}: 200 nm Center	z_{max}: 10 nm Center
Growth Temperature 383°C Growth Rate in the Dark 0.51 μm/ hr	z_{max}: 100 nm Center	z_{max}: 100 nm Center z_{max}: 100 nm 35 μm from Center	z_{max}: 30 nm Center
Growth Temperature 421°C Growth Rate in the Dark 0.84 μm/ hr	z_{max}: 10 nm Center	z_{max}: 5 nm Center	z_{max}: 5 nm Center

Dimensions:

y, x: 1 μm, 1 μm

z z_{max}

z_{max} / 2

0

Scan Location: as indicated on image
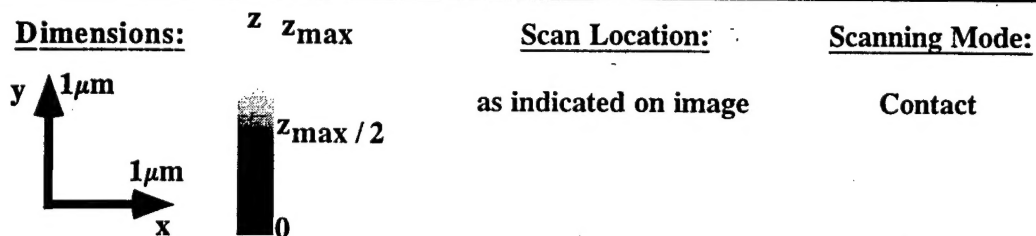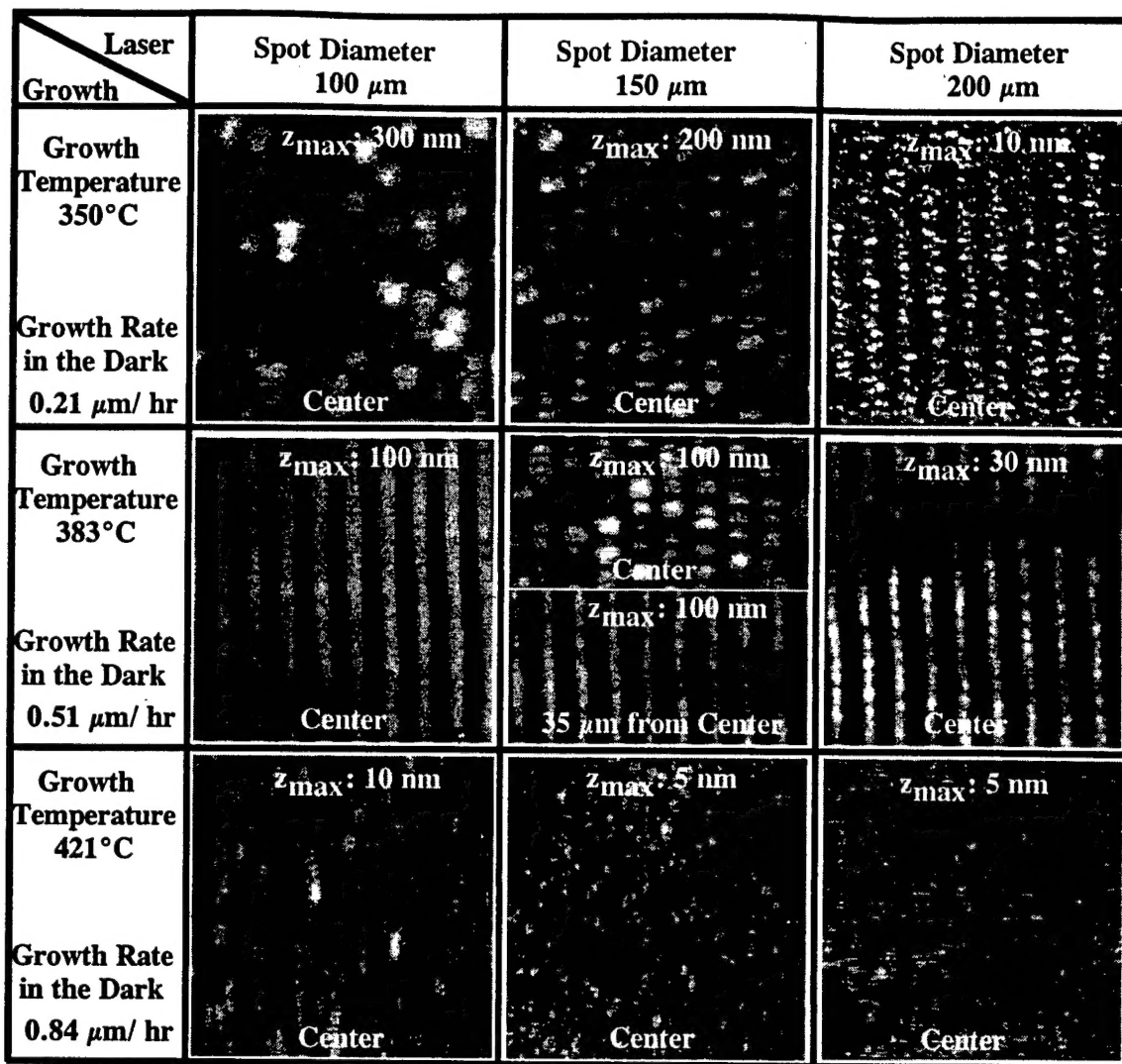
Scanning Mode: Contact

Figure 3. AFM images of GaAs laser stimulated spots grown for 2 min. and under conditions as indicated. The laser power was 180 mW in all cases.
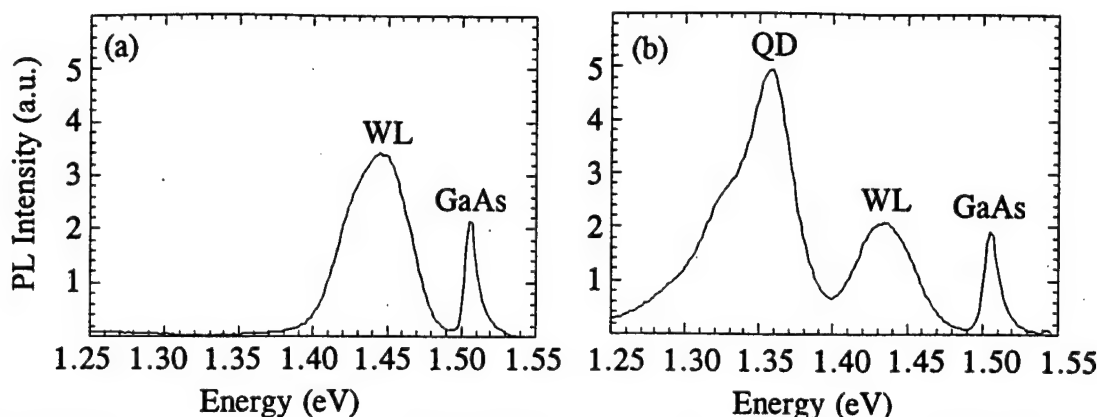
Figure 4. Photoluminescence spectra at 77K of (a) unstimulated region and (b) center of UV laser stimulated region.

SCIENTIFIC IMPACT

We have shown that the composition of AlGaAs grown in the kinetically limited regime depends critically on the V/III ratio due to TMA-arsine adduct formation. Furthermore, the high unintentional carbon doping under these growth conditions affects the photoluminescence wavelength equally through bandgap narrowing and strain. In our UV laser selective growth studies, we determined that photostimulation of the adlayer reaction constitutes the dominant growth enhancement mechanism under pulsed excitation, whereas reaction catalysis through photo-generated carriers is the responsible mechanism under CW laser illumination. Both stimulation mechanisms allow submicron patterning resolution. Self-induced surface periodic structures were observed in both cases, where growth can be controlled to proceed smoothly during CW laser stimulation. The surface morphology is highly sensitive to the combination of laser intensity and dark growth rate. This finding furthered the understanding of the dynamics involved in the positive feedback mechanism responsible for the grating generation. At proper conditions, long range ordered homogeneous submicron gratings can be produced in-situ for potential application in optical devices. Optically active InAs quantum dots have been successfully growth area-selectively with CW laser stimulation.

REFERENCES

[1] V.M. Donnelly, C.W. Tu, J.C. Beggy, V.R. McCrary, M.G. Lamont, T.D.Harris, F.A. Baiocchi and R.C. Farrow, *Appl. Phys. Lett.* , **52** (1988), 1065.

[2] V.M. Donnelly, V.R. McCrary, A. Appelbaum, D. Brasen and W.P. Lowe, *J. Appl. Phys.* , **61** (1987), 1410.

[3] J.-I. Nishizawa, H. Abe, T. Kurabayashi and N. Sakurai, *J. Vac. Sci. Technol.* , **A4** (1986), 706.

[4] T. Farrell, J.V. Armstrong, T.B. Joyce, T.J. Bullough, P. Kightely and P.J. Goodhew, *J. Cryst. Growth* , **120** (1992), 395.

[5] N. Pütz, H. Heinecke, E. Veuhoff, G. Arens, M. Heyen, H. Lüth and P. Balk, *J. Cryst. Growth* , **68** (1984), 194.

[6] P. Balk, H. Heinecke, N. Pütz, C. Plass and H. Lüth, *J. Vac. Sci. Technol.* , **A4** (1986), 711.

[7] P. Balk, M. Fischer, D. Grundmann, R. Lückerath, H. Luth and W. Richter, *J. Vac. Sci. Technol.* , **B5** (1987), 1453.

[8] J. Wisser, P. Czuprin, D. Grundmann, P. Balk M. Waschbüsch, R. Lückerath and W. Richter, *J. Cryst. Growth* , **107** (1991).

[9] V.M. Donnelly and J.A. McCaulley, *Appl. Phys. Lett.* , **54** (1989), 2458.

[10] A. Doi, Y. Aoyagi and S. Namba, *Appl. Phys. Lett.* , **49** (1986), 785.

[11] T.F. Kuech and J.M. Redwing, *J. Cryst. Growth*, **145** (1994), 382.

[12] M. Mashita, *Jap. J. Appl. Phys*, **29** (1990), 813.

[13] J.E. Sipe, J.F. Young, J.S. Preston and H.M. van Driel, *Phys. Rev. B* , **29** (1983), 1141.

[14] J. F. Young, J.S. Preston, H.M. van Driel and J.E. Sipe, *Phys. Rev. B* , **29** (1983), 1155.

[15] A. Barborica, I.N. Mihailescu and V.S. Teodorescu, *Phys. Rev. B*, **49** (1994), 8385.

[16] M. Grundmann, N.N. Ledentsov, O. Stier, J. Böhrer, D. Bimberg, V.M. Ustinov, P.S. Kop'ev, and Zh.I. Alferov, *Phys. Rev. B* , **53** (1996), R10509.

[17] S. Ruvimov, P. Werner, K. Scheerschmidt, U. Gösele, J. Heydenreich, U. Richter, N.N. Ledentsov, M. Grundmann, D. Bimberg, V.M. Ustinov, A.Yu. Egorov, P.S. Kop'ev, and Zh.I. Alferov, *Phys. Rev. B* , **51** (1995), 14766.

JSEP PUBLICATIONS

1. A.Wankerl, D.T. Emerson, M.J. Cook and J.R.Shealy, in *Defects in Electronic Materials II* , eds. J. Michel, T. Kennedy, K. Wada, K Thonke, Mat. Res. Soc. Pro. Vol. 442, pp. 479-484, 1996 (Boston, MA).

2. A. Wankerl, D.T. Emerson and J.R. Shealy, "Sub-Micron Selective Organometallic Vapor Phase Epitaxy Growth Using Deep UV Excitation", Appl. Phys. Lett. **72**, 1614 (1998).

3. A. Wankerl, D.T. Emerson, M.J. Cook and J.R. Shealy, "Wavelength Dependence of UV Laser Selective $Al_xGa_{1-x}As$ Growth via Adlayer Stimulation in OMVPE", J. Cryst. Growth **191**, 8 (1998).

4. A.Wankerl, A.T. Schremer and J.R. Shealy, "Laser Stimulated Selective Area Growth of Quantum Dots", Appl. Phys. Lett. **72**, 3332 (1998).

5. A. Wankerl, D.T. Emerson, M.J. Cook and J.R. Shealy, "Wavelength Tunable UV Laser Stimulated Growth of $Al_xGa_{1-x}As$ by OMVPE", 1997 IEEE International Symposium on Compound Semiconductors, pp. 45-48, 1997 (San Diego, CA).

JSEP PUBLICATIONS IN PROGRESS

1. A.Wankerl, D.T. Emerson, M.J. Cook and J.R.Shealy, "Carbon Incorporation in Low Temperature OMVPE Grown $Al_xGa_{1-x}As$", submitted to J. Cryst. Growth.

2. A. Wankerl and J.R. Shealy "Deep-UV CW Laser Stimulated Organometallic Vapor Phase Epitaxy", to be submitted to Appl. Phys. Lett.

Task #2 BROADLY TUNABLE FEMTOSECOND SOURCES AND ULTRAFAST PROPERTIES OF OPTICAL MATERIALS

Task Principal Investigator: C. L. Tang, (607) 255-5120

OBJECTIVE

The objective of this task is to develop new femtosecond sources and measurement techniques and to apply these to the study ultrafast processes in semiconductors and related quantum well structures. Emphasis has been on applying the high repetition rate all-solid-state femtosecond sources in the important 3 to 5 μm range and the blue-green range first developed in our laboratory to the study of the relaxation dynamics of non-equlibrium carriers in elemental and compound semiconductors and quantum well structures. Main emphasis has been on the dynamics of holes in GaAs in the mid-infrared.

DISCUSSION OF STATE-OF-THE-ART

Development of femtosecond sources has focused on extending the wavelength range of such sources in recent years. With the recent development of femtosecond optical parametric oscillators, which was pioneeded in our laboratory, the accessable spectral range now extends from the near uv to the mid-ir. The quasi-phase-matching technique in nonlinear optical frequency-conversion was initially proposed by Bloembergen and co-workers in the early days of nonlinear optics. The recent development of periodically poled lithium niobate (PPLN) has led to the development of a variety of highly efficient and compact all solid state nonlinear optical devices. Of particular interest are the optical parametric oscillators using PPLN[1] from cw to the nanosecond time domain. We have most recently demonstrated for the first time a highly efficient broadly tunable femtosecond optical parametric oscillator (fs OPO) using PPLN[2]. The threshold for oscillation of PPLN fs OPO is remarkably low, on the order of 60 mW. As a result, it is now possible to use a diode-pumped and frequency-doubled $Nd:YVO_4$ laser, rather than an Ar-ion laser, as the pump source for the mode-locked Ti:sapphire laser which in turn pumps the fs OPO. Such an all-solid-state fs OPO can operate from approximately 1 to 5.4 microns, making this a very useful broadly tunable fs source. The characteristics of the PPLN fs OPO will be summarized and discussed.

There have been numerous studies of the ultrafast dynamics of nonequilibrium conduction band electrons in semiconductors such as GaAs using the femtosecond pump-probe technique in absorption-saturation spectroscopy. Because of the limited wavelength accessibility of early femtosecond sources, both pump and probe transitions tend to involve the same pair of energy bands. Therefore, two types of carriers inevitably contribute to the probe signals in such experiments. To interpret the data, it is often assumed that the excited holes relax quickly to a quasi-equilibrium state and the initial transient characteristics of the probe signal reflect mainly the relaxation dynamics of the excited nonequilibrium electrons. In recent years, there has been much interest in the question of the validity of this basic assumption and in the study of ultrafast relaxation dynamics of the holes independent of those of the electrons in its own right.

To study one type of carriers at a time optically, it is preferable to pump and probe between completely full and completely empty bands. Conduction band electrons near the zone center in GaAs, for example, can be optically excited from the heavy- or light-hole bands using the ~800 nm output of Ti:sapphire femtosecond laser leaving the split-off band completely free of holes. The dynamics of these excited holes can then be probed from the split-off band, which requires tunable mid-ir (~ 3 μm) femtosecond pulses. The Ti:S pumped broadly tunable femtosecond optical parametric oscillators (fs OPO) with precisely synchronized output pulses at multiple wavelengths developed by us are ideal for such a prupose. We have carried out a comprehensive study of the ultrafast dynamics of holes in GaAs using two-photon tunable femtosecond spectroscopy, by pumping the valence-to-conduction band transition at approximately 800 nm and simultaneously probing the transitions between the split-off and heavy- and light-hole bands at around 3 microns. A similar approach has been used very recently by Camescasse et al.[3] to measure the

ultrafast redistribution of electrons created through heavy-hole and light-hole-to-conduction transitions by femtosecond near-IR pulses and probed by visible pulses via the split-off-to-conduction band transition.

The two-wavelength femtosecond pump-probe spectroscopic technique[4,5] described above to study the ultrafast dynamics of heavy- and light-holes (HH and LH, respectively) in GaAs cannot be used to study the dynamics of split-off (SO) holes, however, because direct optical excitation from the SO band to the conduction (C) band will inevitably be accompanied by excitations from the HH and LH bands, leaving no empty band to which the probe pulse can excite holes.

We have recently developed a new approach for studying the ultrafast dynamics of SO holes that also offers new insight into the dynamics of HH and LH. It was shown in fs pump-probe experiments[5] that HH and LH in GaAs come to a quasi-equilibrium distribution in less than a picosecond after the arrival of a fs Ti:S pump pulse. After an initial rapid relaxation period, the C band electron and HH and LH distributions vary very slowly for hundreds of ps, which is orders of magnitude longer than the expected lifetime of the SO holes (~<100 fs). Excitation of holes from such nearly stationary HH or LH distributions to the SO band by fs mid-infrared pulses will lead to induced luminescence due to recombination of the slowly varying C band electron distribution with the SO holes. The time dependence of this mid-infrared-induced luminescence will then reflect the ultrafast relaxation dynamics of the SO holes, which are expected to have lifetimes that are much shorter than the time scale for variations in the C band distribution.

The lifetime of SO holes in GaAs is expected to be very short in part because the density of final states for interband scattering from the SO band to the LH and HH bands is extremely high compared to the density of final states for the reverse processes. Calculations by Scholz[6] indicate that the dominant scattering mechanism for SO holes is the interband deformation potential scattering interaction with optical phonons. The room-temperature lifetime for SO holes, including the effects of polar optical and deformation potential optical and acoustic phonon scattering, was calculated to be ~54 fs.[6] Aronov et al.[7] determined the lifetime of SO holes in highly doped (n-type) GaAs at ~2° K to be 130 fs by measuring the depolarization of luminescence in a transverse magnetic field, and Woerner et al.[8] were able to put an upper limit of ~150 fs on the lifetime of SO holes in p-type Ge at temperatures ranging from 10° to 60° K using a two-wavelength pump-probe experiment. To our knowledge the lifetime of SO holes in GaAs at room temperature has not been studied previously.

PROGRESS

A high-repetion femtosecond optical parametric oscillator that was broadly tunable in the mid-infrared was demonstrated for the first time[2]. The all-solid-state-pumped OPO was based on quasi-phase-matching in PPLN. The idler was tunable from approximately 1.7 μm to beyond 5.4 μm, with maximum average power levels greater 200 mW and approximately 20 mW at 5.4 μm. We used interferometric autocorrelation to characterize the mid-ir pulses, which had typical durations of 125 fs. This OPO had a pump threshold for oscillation as low as 65 mW of average power, maximum conversion efficiency of >35% into the near-ir, a slope effciency for the signal of approximately 60%, and a maximum pump depletion of more than 85%.

We have carried out the first study of the dynamics of holes in GaAs using two-wavelength femtosecond spectroscopy. Ultrafast relaxation dynamics of light and heavy holes in GaAs following femtosecond valence-to-conduction-band femtoscecond excitation were measured by probing the light- and heavy-holes from the split-off band at different mid-infrared wavlengths using the PPLN fs OPO described above. The initial relaxation times are less than 75 fs, and a spectral hole-burning effect is seen. The results suggest that carrier-carrier and optical-phonon scattering, in particular, polar optical-phonon scattering, are the primary processes leading to the initial redistribution of heavy and light holes.

The ultrafast relaxation dynamics of split-off holes in GaAs is studied using a time-resolved two-wavelength excitation luminescence technique. Following conduction-to-valence band transitions that are

excited by near-infrared femtosecond pulses, delayed mid-infrared femtosecond pulses are used to promote holes from the heavy-hole band to the split-off hole band. The subsequent conduction-to-split-off-hole luminescence pulse indicates that the room-temperature lifetime of split-off holes in GaAs is approximately 50 fs. The accompanying reduction in conduction-to-heavy-hole band luminescence when holes are transferred to the split-off band is also observed.

We have also completed a series of measurments on the ultrafast changes in the absorption and refractive index of pure GaAs in the near- and mid-infrared range of the optical spectrum. The multi-color experiments have been performed by using the ultrafast PPLN optical parametric oscillator that allowed photoexcitation of the electron-hole plasma and probing of the associated changes in both parts of the dielectric function in a wide spectral range (~ 1 - 4 μm) with femtosecond time resolution. We found that while the change in aborption is primarily due to resonant intervalence band optical transitions and, therefore, provides information on the dynamics of nonequilibrium holes, the corresponding refractive index change is dominated by the nonresonant contribution due to plasma oscillations of the free carriers. Unlike the dynmaics of the absorption coefficient, the time evolution of the refractive index change is found to be s trongly affected by the procsses of diffusion of free carriers into the bulk of the materal and surface recombination. The latter effect may proceed on picorsecond time scale depending on the surface quality of the samples. We deduced from our measurments that the characterstic surface reconbination velocity constant may be as hight as 7.5×10^5 cm/s.

SCIENTIFIC IMPACT

The tunable femtosecond sources and measurement techniques developed should be of great use to others in the scientific community. The development of a all-solid-state diode pumped femtosecond source in the 1- to 5-μm range is of particular practical importance. The mid-infrared induced luminescence technique developed to study the dynamics of holes in GaAs can be extended to study the relaxation dyanmics of nonequilibrium carriers in a variety of semiconductors and molecules. The results obtained on the dynamics of nonequilibrium carriers in compound semiconductors and structures are of fundamental importance to the understanding of the physics and the design of ultra-high speed semiconductor electronic and optical devices.

REFERENCES

1. W. R. Bosenberg, A. Drobshoff, J. I. Alexander, L. E. Meyers, and R. L. Byer, Opt. Lett. **21**, 1336(1996).
2. K. C. Burr, C. L. Tang, M. A. Arbore, and M. M. Fejer, App. Phys. Lett. **70**, 3341(1997).
3. F. X. Camescasse, A. Alexandrow, D. Hulin, L. Banyai, D. B. Tran Thoai, and H. Haug, Phys. Rev. Lett. **77**, 5429(1996).
4. JSEP Progress Report, 9/1/96 to 8/31/97.
5. F. Ganihkanov, K. C. Burr, and C. L. Tang, App. Phys. Lett. **73**, 64(1998).
6. R. Shcolz, J. App. Phys. **77**, 3219(1995).
7. A. G. Aronov, D. N. Mirlin, L. P. Niktin, I. I. Reshina, and V. F. Sapega, JETP Lett., **29**, 62(1979).
8. M. Woener, and T. Elsasser, Phys. Rev. **B51**, 17490(1995).

DEGREES AWARDED

Benjamin B. Jian, "Design and fabrication of a monolithic two-mode optical flip-flop", Ph.D., January, 1997.

Scott F. Pesarcik, "Etched-Angled-Facit Superluminescent Diodes for Improved Mode-Locking", Ph. D., May, 1998.

JSEP PUBLICATIONS

1. "High average power, high repetition rate femtosecond pulse generation in the 1 - 5μm region using an optical parametric oscillator", D. E. Spence, W. Wielandy, C. L. Tang, C. Bosshard, and C. L. Tang, App. Phys. Lett., **68**, 452 - 454(1996).

2. "Broadly tunable mid-infrared femtosecond optical parametric oscillator using all-solid-state-pumped periodically poled lithium niobate", K. C. Burr, C. L. Tang, M. A. Arbore, and M. M. Fejer, Optics Letters, **22**, 1458(1997).

3. "High-repetition rate femtosecond optical parametric oscillator based on periodically poled lithium biobate", K. C. Burr, C. L. Tang, M. A. Arbore, and M. M. Fejer, App. Phys. Lett. **70**, 3341-4433(1997).

4. "Tutorial on optical parametric processes and devices", C. L. Tang, J. of Nonlinear Optical Physics and Materials, **6**, 535-547(1997).

5. "Broadly tunable femtosecond sources in the mid-infrared and two-wavelength ultrafast spectroscopy of holes in GaAs", Proc. of XII International Conference on laser spectroscopy, ed. Z-J. Wang Z-M. Zhang, and Y-Z. Wang, Hangzhou, China, 2-7 June, 1997, (published by World Scientific).

6. "Ultrashort-pulse phenomena", C. L. Tang, Encyclopedia of Applied Physics, **22**, 457-473(1998 Wieley-VCH Verlag GmbH).

7. "Broadly tunable femtosecond sources in the mid-infrared and two-wavelength ultrafast spectroscopy of holes in GaAs", C. L. Tang, K. C. Burr, and F. Sh. Ganihkanov, J. of Nonlinear Optical Physics and Materials, **7**, 61-71(1998).

8. "Ultrafast dynamics of holes in GaAs probed by two-color femtosecond spectroscopy", F. Ganikhanov, K. C. Burr, and C. L. Tang, App. Phys. Lett. Vol.73 , 64(1998).

JSEP PUBLICATIONS IN PROGRESS

1. "Optical parametric processes in crystals", C. L. Tang, *Encyclopedia of Materials Science and Technology*, Sec. 6.8 , ed. D. D. Nolte, Elsevier Science Ltd., Oxford, England, (to be published).

2. "Femtosecond optical pulse induced absorption and refractive index changes in GaAs in the mid-infrared", F. Ganihkanov, K. C. Burr, D. J. Hilton, and C. L. Tang (submitted to Physical Review **B**).

3. "Switching dynamics of vertical-cavity surface-emitting lasers by injection of femtosecond optical pulses", D. Fortusini, K. C. Burr, F. Robert, and C. L. Tang (submitted to App. Phys. Lett.).

RELATED PUBLICATIONS

1. "Coupled in-plane and vertical-cavity lasr 1XN routing switches", D. B. Shire, C. L. Tang, M. Hong, and J. D. Wynn, Photonics Tech. Letters, **8**, 1537(Nov., 1996).

2. "Bistable operation of coupled in-plane and oxide-confined vertical cavity laser 1xN routing switches", D. B. Shire, C. L. Tang, M. A. Parker, C. Lei, and L. Hodge, App. Phys. Lett. **71**, 3039(November 24, 1997).

3. "Laser Polarization self-modulation effects" , C.L. Tang, Quantum and Semiclassical Optics, Journal of the European Optical Society - Part B for the Topical Issue on Polarization Effects in Lasers and Spectroscopy, Neal Abraham, Guy Stephan - Guest Editors, Vol. 10, R51(February, 1998).

4. "Laser polarization self-modulation effects", C. L. Tang, Quantum Semiclass.Opt. 10(1998), R51 - R58.

PRESENTATIONS

1. "Monolithically - integrated semiconductor 1:N router or space-division switch with time-division multiplexing and demultiplexing capability", D. B. Shire, C. L. Tang, and M. H. Hong, CLEO Post Deadline paper, Anaheim, CA (June 5, 1996).

2. "Applications of nonlinear optical materials to fs OPO's", invited plenary talk, Center for Nonlinear Optical Materials Annual Affliliates Meeting, Stanford University, Palo Alto, CA , September 17, 1996.

3. "Recent developments in femtosecond optical parametric generators", invited talk, ThT1, Optical Society Annual Meeting, Rochester, NY, September 20, 1996.

4. "Optical parametric processes and broadly tunable femtosecond sources", invited talk, Khokhlov Tutorials at the 70th Khokhlov Jubilee, Moscow University, Moscow, Russia, October 14- 19, 1996.

5. "Femtosecond optical parametric oscillators and two-wavelength ultrafast laser spectroscopy of holes in GaAs", invited talk, 13th International Conference on Laser Spectroscopy, June 2, 6, 1997, Hangzhou, China.

6. "Femtosecond optical parametric sources in the mid-infrared and ultrafast dynamics of holes in GaAs", invited talk, Novel Optical Materials and Applications - NOMA '97, June 8 - 13, 1997, Cetraro, Italy.

7. "Polarization self-modulation in semiconductor lasers", invited talk, First International Conference ans School on Polarization Efftects in Lasers and Spectroscopy - Fundamentals and Applications, Toronto, Canada, May 26 -28, 1997.

8. "Ultrafast dynamics of holes in GaAs probed by two-color femtosecond spectroscopy", F. Ganikhanov, K. C. Burr, and C. L. Tang, IQEC '98, May 5, 1998, Anaheim, CA.

9.   "Femtosecond optical parametric sources in the mid-infrared and ultrafast dynamics of holes in GaAs", invited talk, Laboratoire d'Optique Quantique, CNRS, Ecole Polytechnique, Palaiseau, France, March 25, 1998.

10. "Bistable operation of coupled in-plane/oxide-confined VCSEL 1xN routing switches", invited talk, University of Pavia, Pavia, Italy, April 6, 1998.

11. "Femtosecond Optical Parametric Sources in the Mid-Infrared and Ultrafast Dynamics of Holes in GaAs", C. L. Tang, invited Plennary Talk, Photonics Technology, SPIE meeting, July 12, 1998, Taipei, Taiwan.

12. "Femtosecond optical parametric oscillator in the mid-infrared and the dynamics of holes in GaAs", F. Ganikhanov, K. C. Burr, and C. L. Tang, FB1, Nonlinear Optics '98, Kauai, Hawaii, August 10-14, 1998.

13. "Switching and dynamic interconnects using optically controlled vertical-cavity surface emitting lasers", C. L. Tang, F. Robert, and C. B. Shire, invited talk T08, 1998 international conference on Applications of Photonic Technology, Ottawa, Canada, July 27- 30, 1998.

Task #3 CONTROLLING CHAOS IN LASERS AND FEMTOSECOND CHARACTERIZATION OF SEMICONDUCTOR DEVICES

Principal Investigator: Clifford Pollock, (607) 255-5032

OBJECTIVES

We pursued two projects relevant to the Air Force mission: controlling chaos in lasers, and developing tunable lasers for the 3-5 micron region. We explored the control of chaos in a single laser to create a rich source of complex frequencies for applications such as secure communications, and to apply the control techniques to semiconductor laser arrays. Our short-term goal was to develop chaos control techniques on an additive pulse modelocked laser based on the NaCl color center laser. The long-term goal was to apply these techniques to semiconductor lasers. Specifically we characterized the bifurcation diagram and the chaotic attractors for the additive pulse modelocked laser. We were not able to explore the chaos studies with semiconductor lasers.

We studied the creation of solid state laser crystals for use as tunable sources in the 3-5 micron region. $Cr2+$ in chalcoginate crystals have been shown by workers at the Lawrence Livermore National Laboratory to lase in this near-infrared region. We developed techniques to diffuse Cr into relatively inexpensive ZnSe crystals, and have exploring lasers based on our diffused crystals. Our objective was to create an effective means to produce the crystal, and to explore pumping and modelocked operation of the crystals. We succeeded in making good quality laser crystals, and have tentative modelocking results.

DISCUSSION OF STATE-OF-THE-ART

In 1990, Ott, Grebogi, and Yorke (OGY) [1] at the University of Maryland demonstrated that chaotic systems can be controlled by means of small steering perturbations. Small, judiciously chosen temporal parameter perturbations are applied to force the system to approach the desired unstable periodic orbit. The OGY algorithm was first implemented experimentally by Ditto[2] at the Naval Surface Warfare Center in order to control the chaotic behavior in a magnetoelastic ribbon vibrating at 0.85Hz. Due to the long oscillation period, there was ample time to calculate by computer the required feedback factor. Experimentally, it is complicated and time consuming to calculate the OGY-required perturbations necessary to stabilize the unstable periodic orbits. Hunt at Ohio University [3] successfully adapted the OGY algorithm using a technique known as occasional proportional feedback (OPF) to control a 53kHz sine-wave-driven diode resonator.

Using Hunt's OPF technique, Roy [4] at Georgia Tech controlled chaos in a diode-laser-pumped Nd:YAG laser which contains a KTP crystal in the cavity as a second harmonic generator. The controlling feedback was obtained by sampling the lasers output intensity and modulating the control signal to the diode laser pump. In this manner, orbits up to period 9 were stabilized for durations of several minutes. Bielawski et al.[5] stabilized the unstable periodic orbits in a Nd-doped optical fiber laser that was operating at 15kHz.

Pyragas [6] showed that low period UPOs could be stabilized by continuously applying time-delayed feedback. This scheme has also been applied by Glorieux et al. [7] in order to control unstable periodic orbits in a carbon dioxide laser that typically operates at the relaxation oscillation frequency of 400 kHz. This was accomplished by modulating an intracavity electro-optic modulator with the constantly amplified difference between the output intensity and the one period delayed intensity.

Extending chaos studies to higher frequencies has been one of the driving themes of this work. Mitschke et. al. [8] have done work the most similar to what we list in this report. An Additive Pulse Modelocked laser provides a nonlinear system that is noted for operating in chaotic states. Using a Nd:YAG laser, they observed period doubling behavior with an APM laser. Their work was not supported by a model of the chaotic laser.

Tunable IR lasers: Progress in developing tunable lasers in the 3-5 micron region has been very slow for the past decade. In the '80s there was great hope that color center lasers would fill this gap, yet the ability to create stable lasers based on color centers in alkali halides proved impractical. In 1996, DeLoach et. al [9] demonstrated a new class of laser based on Cr2+ doped into zinc chalcogenides. Cr:ZnSe has been the most actively developed laser of this class, with a room temperature tuning range spanning 2.13 - 2.80 microns. Page[10] demonstrated pulsed operation of this laser using a laser diode pump operating at 1.65 micron, and recently Carrig et al.[11] demonstrated strong cw lasing using a Tm pump laser. Extending the tuning range toward longer wavelengths, Adams et al [12] demonstrated Fe-doped ZnSe laser tunable in a narrow region around 3.98 micron.

PROGRESS

The controlled chaos work was primarily performed by Eric Mozdy, a JSEP fellow. In this work we used an additive-pulse modelocked laser as a nonlinear system that could be manipulated to display chaotic operation. In order to systematically observe the chaotic operation of the laser, several advances in APM technology had to first be achieved. We first systematically improved the modelocking techniques used to initiate the APM laser, then we used the improved lasers to make experimental observations bifurcation diagrams. These are summarized below in the order of publication.

Saturable Bragg Reflector Modelocked NaCl:OH⁻ Color Center Laser [IEICE Trans. Electron. Vol. E81-C, February 1998, pp.125-128] [13]

The additive pulse mode-locked laser used in these experiments provides a rich source of chaotic behavior for observation, but unfortunately it was hampered by multiple instabilities, such as a "sawtooth" amplitude feature due to the asynchronicity of the self-modelocking frequency and of the mode-locked pump laser. Since the chaotic behavior we were seeking appears as amplitude variations, the sawtooth was a serious noise source. The best solution for eliminating it was to use a cw pump, but this then eliminated the starting mechanism that maintained the APM operation. Based on recent results using Ti:Sapphire lasers [12], we decided to try using a saturable absorber based on quantum wells grown over a Bragg reflector in order to sustain the modelocked operation of the NaCl laser.

We had developed an SBR for a Cr:YAG laser in collaboration with Mike Hayduk at Rome Laboratory [20]. This SBR was designed to work at 1.52 µm, which was within the tuning range of the APM laser. The cavity was configured as shown below in fig. 1. The SBR was used as a high reflector on one end of the cavity. A focussing mirror was used to boost the intensity of the mode on the SBR.
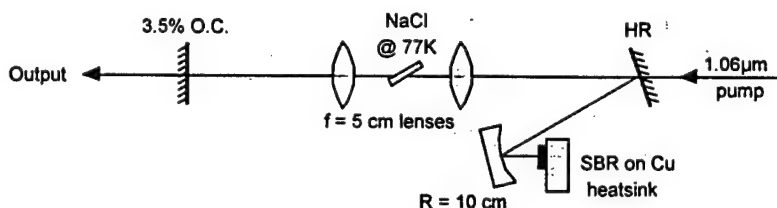

Fig. 1. The NaCl SBR modelocked laser

Fig. 2 shows a sample output pulse autocorrelation and corresponding spectrum of a 233 fs (sech^2) pulse, yielding a 0.33 time-bandwidth product. In contrast to regular APM operation, this laser was self-starting even when pumped by a cw laser, and needed no active or passive adjustment to maintain operation.
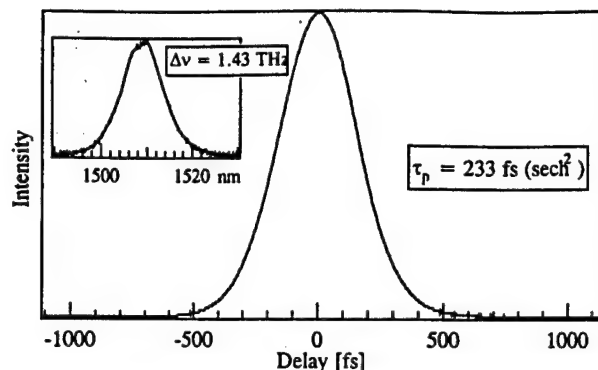
Fig. 2 Sample pulse autocorrelation and spectrum of a 23 fs pulse from a NaCl SBR laser.

The tuning range for this laser was limited by the spectral reflectivity of the Bragg grating, but was found to deliver transform limited pulses from 1.499 to 1.535 µm. The stability of this laser provided a dramatic advance in the utility of modelocked color center lasers lasers.

NaCl:OH- Color Center Laser Modelocked by a Novel Bonded
Saturable Bragg Reflector [Optics Communications, 151, pp.62-64 (1998)] [14]

The SBR used to generate the data in Figs. 1 and 2 was grown specifically for a Cr:YAG laser, and so our ability to extend the tuning range to new regions was limited by our lack of new SBRs. In collaboration with Prof. Yu Hwa Lo of this JSEP program, we developed a new type of SBR based on bonded quantum well absorbers. Prof. Lo's work was on VCSEL lasers using bonded structures. Part of his experimental procedure was to grow a set of quantum well appropriate for the wavelength he needed, and then subsequently he would bond the high reflector and output coupler to the form the VCSEL. Since his VCSEL work was focussed in the 1.55 µm spectral region, we used one of his quantum well structures to form an SBR. The QW stack was bonded to a Bragg reflector grown to match the QW emission, and this was used as an SBR in our cavity. The cavity structure is identical to that shown in Fig. 1. The bonded SBR provided much higher output power, which we attribute to a better Brag reflector, and it was much more robust in mode-locking, which we attribute to the deeper modulation created by the increase in QW compared to our first SBR. A sample output pulse is shown in fig. 3.
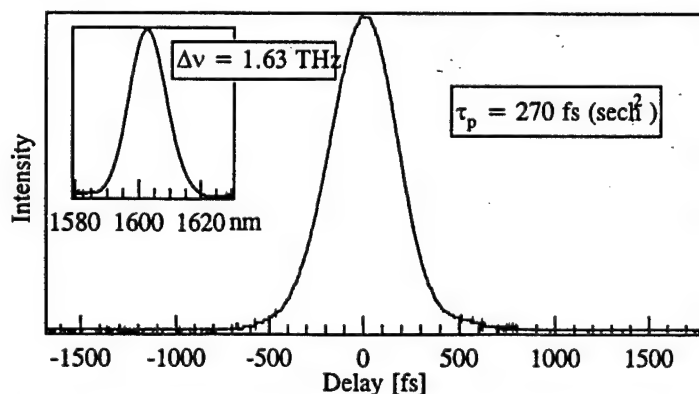

Fig. 3 Pulse autocorrelation and spectrum of a typical bonded SBR NaCl laser.

The time-bandwidth product for the pulse shown in fig. 3 is 0.44, indicating it has a slight chirp. Like the SBR laser in the previous section, the laser was self-starting and very stable, providing up to 500 mW of output power. Not only was the performance improved over the previous SBR design, but the bonded SBR demonstrated the ability to use widely-available VCSEL QW structures to make SBRs for various wavelengths. The cost of a dedicated growth run to make an SBR is prohibitive for small users, but the comparatively large number of VCSEL components being generated at numerous wavelengths in the 1.3 and 1.5 µm spectral region opens the possibility that a user can find a useful device.

Self-starting of an additive-pulse modelocked laser using a novel bonded saturable Bragg reflector, [IEE Electronics Letters, vol. 34, pp. 1497 (1998)] [15]

The main purpose of the SBR was to provide self-starting for the APM cavity, so as to eliminate the gain modulation that always occurred when pumping asynchronously with a modelocked laser. Fig. 4 shows the cavity for the SBR/APM laser. The only modification is the addition of 40 centimeters of single mode fiber into an external cavity of the laser. The length of the external cavity is precisely matched to that of the primary cavity.
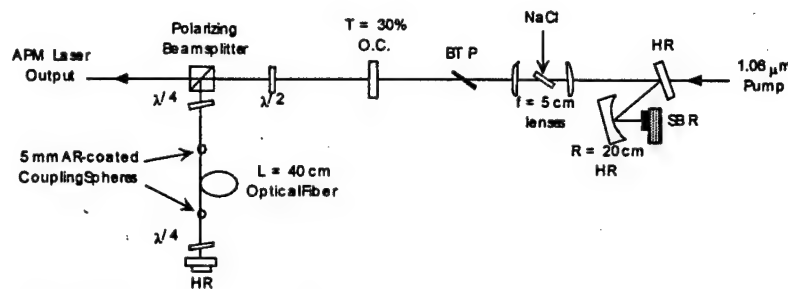

Fig. 4 The hybrid SBR/APM laser cavity, which is simply an alteration of the APM laser to include the SBR device.

An autocorrelation trace of the output of the SBr/APM laser is shown in fig. 5. This autocorrelation is un-averaged and in fact represents the free-running APM operation, meaning that no cavity length stabilization was employed. This feature is critical for the chaos studies described below.
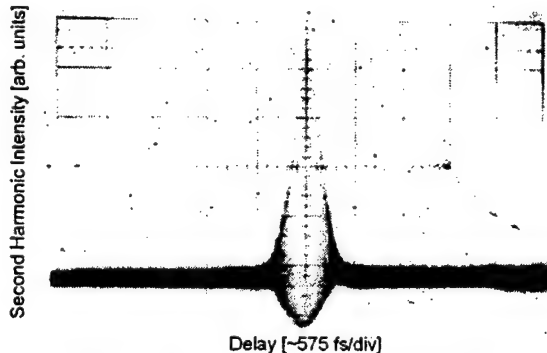

Fig. 5 Interferometric autocorrelation of the free-running hybrid APM laser, displaying the exceptionally clean baseline devoid of all sawtooth behavior.

Deterministic generated noise amplification in the period-doubling bifurcations of an additive-pulse modelocked laser, [Physics Letters A 249, pp. 218-222, (1998)] [15]

Theoretical simulations of chaos demonstrate the sensitivity of small perturbations to the long-term dynamics of a system, but these simulations are difficult to verify experimentally due to the presence of noise. Crutchfield [16] studied the impact of noise on the period-doubling route to chaos. His central finding was that additive noise tends to blur the features in bifurcation diagrams and attractors, and tends to destroy some of the higher periodicities in the bifurcation diagram. The impact of these studies to our APM chaos studies was that we should expect to see a lot of detail or high-period orbits in the experimental data. This was born out in the data. Several groups [17] have studied noise in general and found that the steady state noise power spectrum acquires a well-defined peak at the period-two oscillation frequency. This noise is much greater than the original source, and is deemed an amplification of the noise.

We observed a noise-induced period-two behavior, but it was in fact more complex than predicted by others [17]. We tuned the laser to a period-one region, and observed the noise power spectrum. In this condition a weak period-two oscillation can be seen using a spectrum analyzer. Far from the bifurcation point, the period-two-like frequency appears slightly below the true period-two frequency for the pulses. As the bifurcation parameter moved closer to the bifurcation point, the frequency was pulled closer to the true period-two frequency, culminating in actual bifurcation. The power spectra below show the size and evolution of the pulse as the bifurcation point is approached.
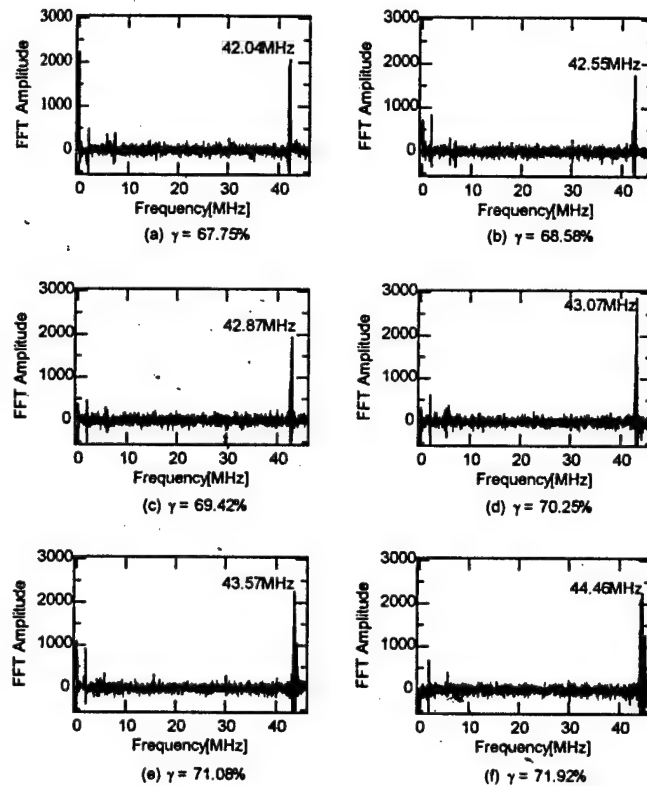

Fig.6 The progression of "period-two noise" in the period-one APM output. The actual noise starts below the natural period-two frequency (45.68 MHz in this case), then comes closer as bifurcation is approached. (a) is furthest from bifurcation, and (f) is closest.

We found that the strength and magnitude of the frequency pulling could be modeled by invoking multi-path feedback due to reflections from external components. This model was developed by Park[18] to describe self pulsing in semiconductor lasers with external cavities.

Chaos in additive-pulse modelocked lasers [19]

By experimentally varying the forward fiber coupling while recording a time series of APM output pulse energies, we produced the first experimental bifurcation diagram for the APM laser. This bifurcation diagram clearly demonstrated both quasi-periodic behavior as well as the period-doubling route to chaos predicted by the numerical simulations of previous work[19]. The bifurcation plot is shown in Fig. 7 attached to the next page, as a function of coupling parameter, γ.

We performed both graphical and a more quantitive (prediction) analysis on the chaotic time series data to ensure that the output was indeed chaotic and compared favorably with the APM model. By incorporating simple additive noise into the APM model simulations, we were able to show that the experimental "white"

noise contribution to APM instabilities is on the order of only 0.7%. The bifurcation diagram shown here is one of many possible diagrams, since several APM parameters (relative cavity phase, gain, fiber length) can cause period-doubling bifurcations into chaos. By demonstrating the typical APM route to chaos however, this work confirms the accuracy of the traditional iterative APM model [18] and indicates the APM laser as a useful platform for further nonlinear dynamics study.

Cr:ZnSe Laser

We have just recently obtained the first lasing from one of our Cr:ZnSe laser crystals when pumped with a color center laser at 1.65 μm. With 1.3 W of input pump power, we were able to generate 200 mW of tunable output power from the 2.2 mm thick ZnSe crystal. The crystal is a relatively inexpensive polycrystalline ZnSe window that was doped via an additive coloration process where the crystal is suspended in the vapor of CrSe. The crystal was heated for 5 days at 800 degrees C at atmospheric pressure. These results are not new, as others have demonstrated c lasing with this material, but it does confirm that we can now do it, and puts on the path to develop,this system. We have tentative results with modelocking the laser using an acousto-optic modulator, however due to the lack of high speed instrumentation in the 2.5 μm region, we can only confirm that the pulses were shorter than 300 psec. We also used a modelocked color center laser to sync pump this system, and got a similar result.

We are still working on this crystal. With a few simple optics we will be able to accurately measure the pulse width of the modelocked laser output. Next on the agenda is to dope ZnSe with Fe, which will provide a laser source at 4 μm.

SCIENTIFIC IMPACT

In this work we were able to advance the state-of-the-art of modelocked lasers in the near infrared region through saturable Bragg reflector techniques. These methods of modelocking femtosecond lasers are being adapted and applied to numerous lasers, and has advanced the technology of femtosecond pulse production from solid state lasers. We were able to experimentally map out a bifurcation diagram for a modelocked laser, and this was one of the first experimental observations of such a process. Finally, we are advancing the state of the art in mid-IR tunable lasers, which has the potential of making the first practical and deployable counter-measure lasers for defense use.

REFERENCES

1. E. Ott, C. Grebogi, and J. A. Yorke, "Controlling Chaos," Phys. Rev. Lett. 64, 1196 (1990)

2. W.L. Ditto, S.N. Rauseo, and M.L. Spano, "Experimental Control of Chaos," Phys. Rev. Lett. 65, 3211 (1990)

3. E. R. Hunt, "Stabilizing High-period Orbits in a Chaotic System: the Diode Resonator," Phys. Rev. Lett. 67, 1953 (1991)

4. R. Roy, T.W. Murphy, T.D. Maier, Z. Gills and E.R. Hunt, "Dynamical Control of a Chaotic Laser: Experimental Stabilization of a Globally Coupled System," Phys. Rev. Lett. 68, 1259 (1992)

5. S. Bielawski, D. Derozier, and P. Glorieux, "Experimental characterization of unstable periodic orbits by controlling chaos," Phys. Rev. A 47, R2492 (1993)

6. K. Pyragas, "Continuous control of chaos by self-controlling feedback," Phys. Lett. A, 170, 421 (1992)

7. S. Bielawski, D. Derozier, and P. Glorieux, "Stabilization and characterization of unstable steady states in a laser," Phys. Rev. A 47, 3276 (1993)

8. U. Morgner, L. Rolefs, and F. Mitschke, "Dynamic instabilities in an additive-pulse modelocked Nd:YAG laser," Optics Lett. 21 (1996)

9. R. H. Page, K. I. Schaffers, L. D. DeLoach, G. D. Wilke, F. D. Patel, J. B. Tassano, S. A. Payne, W. F. Krupke, K. T. Chen and A. Burger, "Cr2+ doped zinc chalcogenides as efficient, widely tunable mid-infrared lasers," IEEE J. Quantum Elec. 33, 609-619 (1997)

10. R. H. Page, J. A. Skidmore, K. I. Schaffers, R. J. Beach, S. A. Payne, and W. F. Krupke, "demonstration of a diode-pumped and grating tuned ZnSe:Cr2+ laser," in OSA Trends in Optics and hotonics, vol. 10, Advanced Solid State Lasers, C. R.Pollock and W. R. Bosenberg, eds., pp208-210

11. Gregory J. Wagner, Timothy J. Carrig, Ralph H. Page, Kathleen I. Schaffers, Jean-Oliver Ndap, Xiaoyan Ma, and Arnold Burger "Continuous-wave broadly tunable Cr2 + :ZnSe laser," Optics Letters 24, 19 (1999)

11. J. J. Adams, C. Bibeau, S. A. Payne, and R. H. Page, "Tunable laser action at 4.0 microns from Fe:ZnSe," Procedings of the Advanced Solid State laser Conference '99, Boston, MA (Optical Society of America)

12. B. C. Collings J. B. Stark, S. Tsuda, W. H. Knox, J. E. Cunningham, W. Y. Jan, R. Pathak, and K. Bergman, "Saturable Bragg reflector modelocking of Ti:sapphire Lasers," Optics Lett. 21, 1171 1996)

13. Martin A. Jaspan, Eric J. Mozdy, Clifford R. Pollock, Michael J. Hayduk, and Mark F. Krol, "Saturable Bragg Reflector Modelocked NaCl:OH- Color Center Laser," IEICE Trans. Electron. Vol. E81-C, February 1998, pp.125-128

13. E. J. Mozdy, M. A. Jaspan, Zuhua Zu, Yu-hwa Lo, and C. R. Pollock, R. Bhat,and Minghwei Hong, "NaCl:OH- Color Center Laser Modelocked by a Novel Bonded Saturable Bragg Reflector," Optics Communications, 151, pp.62-64 (1998)

14. E. J. Mozdy and C. R. Pollock, "Self-starting of an additive-pulse modelocked laser using a novel bonded saturable Bragg reflector" IEE Electronics Letters, vol.34, pp. 1497 (1998)

15. E. J. Mozdy and C. R. Pollock, "Deterministic generated noise amplification in the period-doubling bifurcations of an additive-pulse modelocked laser," Physics Letters A 249, pp. 218-222, (1998)

16. J. P. Crutchfield and B. A. Huberman, "Fluctuations and the onset of chaos," Physics letters 77A, 407-410 (1980)

17. J. Garcia-Ojalvo and R. Roy, "Noise amplification in a stochastic Ikeda model," Physics Letters A, 224, 51-56 (1996)

18. J. D. park, D. S. Seo, and J. G. McInerney, "Self-pulsations in strongly coupled asymmetric external cavity semiconductor lasers," IEEE Journal of Quantum Electronics 26, 21353-1362 (1990)

19. E. J. Mozdy and C. R. Pollock, "Chaos in additive-pulse modelocked lasers," submitted to Optics Letters (June, 1999)

20. M. J. Hayduk, S. T. Johns, M. F. Krol, C. R. Pollock, R. P. Leavitt, "Self-starting passively modelocked tunable femtosecond Cr4+:YAG laser using a saturable absorber mirror," Optics Communications 137, pp. 55-58 (1997).

DEGREES AWARDED

Michael J. Hayduk, PhD, Electrical Engineering, August, 1997
"Passively modelocked erbium-doped fiber lasers using multiple quantum well saturable absorbers"

Eric J. Mozdy, PhD, Electrical Engineering, May 1998
"Chaos in the additive-pulse modelocked laser"

Martin Jaspan, PhD, Electrical Engineering, August, 1999
"Saturable Bragg reflector mode-locking of tunable lasers"

JSEP PUBLICATIONS

1. M. J. Hayduk, S. T. Johns, M. F. Krol, C. R. Pollock, R. P. Leavitt, "Self-starting passively modelocked tunable femtosecond Cr4+:YAG laser using a saturable absorber mirror," Optics Communications 137, pp. 55-58 (1997)

2. E. J. Mozdy and C. R. Pollock, "Nonlinear dynamics of the additive-pulse modelocked laser," Discrete Dynamics in Nature and Society, Vol. 2, pp. 99-110 (1998)

3. E. J. Mozdy, M. A. Jaspan, Zuhua Zu, Yu-hwa Lo, and C. R. Pollock, R. Bhat,and Minghwei Hong, "NaCl:OH$^-$ Color Center Laser Modelocked by a Novel Bonded Saturable Bragg Reflector," Optics Communications, 151, pp.62-64 (1998)

4. Martin A. Jaspan, Eric J. Mozdy, Clifford R. Pollock, Michael J. Hayduk, and Mark F. Krol, "Saturable Bragg Reflector Modelocked NaCl:OH- Color Center Laser," IEICE Trans. Electron. Vol. E81-C, February 1998, pp.125-128

5. E. J. Mozdy and C. R. Pollock, "Self-starting of an additive-pulse modelocked laser using a novel bonded saturable Bragg reflector," IEE Electronics Letters, vol.34, pp. 1497 (1998)

6. E. J. Mozdy and C. R. Pollock, "Deterministic generated noise amplification in the period-doubling bifurcations of an additive-pulse modelocked laser," Physics Letters A 249, pp. 218-222, (1998)

JSEP PUBLICATIONS IN PROGRESS

1. E. J. Mozdy and C. R. Pollock, "Chaos in additive-pulse modelocked lasers," submitted to Optics Letters (June, 1998)

TASK #4 LASER PHYSICS FOR LONG WAVELENGTH HIGH-SPEED APPLICATIONS

Principal Investigator: J. Peter Krusius, (607) 255-3401

OBJECTIVE

The original objective of this task was to explore the physics of long wavelength, especially at 1.3μm and 1.55μm, and ultra-fast lasers based on compound semiconductor materials. However, due to the JSEP phase-out and reduced resources, the objectives were changed and completion the ongoing study of fundamental optical processes and carrier relation remained the highest priority. This work has been based on an extensive understanding of the fundamental physics of the optical processes and carrier dynamics in compound semiconductor devices, which was provided by self-consistent Ensemble Monte Carlo (EMC) simulation in combination with femtosecond dual-pulse correlation spectroscopy. In order to describe the complexity of the physical processes in detectors and lasers, an attempt has been made to incorporate all the important physical phenomena involved, including band structure, quantization, lattice strain, carrier dynamics, carrier confinement, Auger recombination, inter-band absorption, optical gain, and carrier and lattice heating in state-of-the-art strained multi-quantum-well laser structures. The investigation has been conducted in collaboration with materials, optical measurement, and device fabrication tasks of this program.

DISCUSSION OF STATE-OF-THE-ART

Although optical communication systems have achieved remarkable success over the past few decades, the development of critical optoelectronic devices such as optical sources, optical amplifiers, and photodetectors still faces challenges. These include: higher signal to noise ratio, greater bandwidth or higher operation speed, higher quantum efficiency, lower power consumption and thermal stresses, easier fabrication and integration, greater compatibility, smaller size, and better linearity for analog applications. A further challenge is to integrate as much as possible the various desired improvements into optimal devices.

Carrier confinement in active region largely determines the quantum efficiency and power dissipation in semiconductor lasers and light emitting diodes (LED). Vertical confinement can be realized by schemes such as homojunctions, heterojunctions and single, or multiple, quantum wells. Two-dimensional quantum wire confinement has also been considered. Lateral current confinement has been attempted and is generally more difficult to achieve. Both LED's and semiconductor lasers suffer from quantum noise resulting from the statistical nature of carrier recombination. Lasers also exhibit modal noise, such as mode-partition noise in multimode lasers or jumping between modes in single mode lasers. Modal noise can be reduced by limiting the lateral and transverse modes by optical confinement and by using wavelength-dependent mirrors, such as Bragg reflectors to limit the operation to a single longitudinal mode. The modulation bandwidth of an LED is determined primarily by the carrier recombination time in the active region, because their structure does not provide any transport mechanisms to sweep the carriers out of the active region. Thus, high-speed modulation can only be achieved at the expense of high power operation. The modulation bandwidth in semiconductor lasers is ultimately limited by the relaxation oscillations of the laser field. This limits present laser modulation bandwidths to about 30 GHz. Ease of integration and better compatibility with electrical devices, and more efficient coupling have become more and more important. VCSEL's (Vertical Cavity Surface Emitting Lasers) excel in these respects over the more conventional edge emitting lasers, especially in array and single mode operation applications.

State-of-the-art optoelectronic sources and amplifiers, such as VCSEL's, incorporate a number of sophisticated structures including heterojunctions, quantum wells, and dielectric mirrors to provide simultaneous electrical and optical confinement. The physics of carrier transport and optical processes in such structures is very complex and is generally not, especially in quantum structures, fully understood. In

particular, inhomogeneities in carrier distribution functions have significant effects on laser performance. Hole burning in the carrier distribution functions and carrier heating have been shown to contribute nonlinear terms to the laser gain [1-2], while spatial hole burning can contribute to laser instability [3]. The index of refraction, and the fundamental band gap are functions of the distribution of carriers both inside and outside the active region. This affects both the gain and the width of the laser line [4-6]. It has been found via simulation that complex structures such as heterojunctions and quantum wells lead to the formation of space charge layers and large electric fields that have serious consequences for both the static and dynamic operation of the device [7]. These effects will also significantly affect all device characteristics from microscopic carrier distribution functions to macroscopic device parameters.

Many theoretical models for use in the design and optimization of photonic semiconductor sources exist. However, in past models the emphasis has been on the optical physics, while the complexities of carrier transport and device physics mentioned above have been de-emphasized or even neglected. These include models based on transmission lines [8-9], the circuit approach [10], coupled-wave theory [11], density matrix formulation [2,12] and rate equations [13-15]. In some of these models the optical aspects are quite sophisticated, but the rest of the device physics is highly simplified. In each of these cases the physics of the gain media is modeled by simple rate equations. Usually the details of the carrier transport, space charges, and distribution function effects are almost completely neglected. Even in models which treat carrier transport within the drift-diffusion formalism in one or two dimensions [16], many complex physical phenomena such as non-equilibrium carrier transport, spatial inhomogeneities, non-thermal carrier distributions resulting from hole burning, are not treated to their due importance.

The ability to accurately describe all significant aspects of the physics of optoelectronic devices is severely limited in published models. Moreover, highly non-equilibrium conditions and many-body effects play a much more prominent role in ultra-fast lasers and need to be addressed from the microscopic level. Therefore it was necessary to simultaneously study both the optical and electronic aspects of device operation down to very short time scales (10fs) and to very small device dimensions (100nm). We have worked on a theoretical model based on sound first principles and backed by experimental verification [17, 18]. Such a first-principle approach can also provide information about the fundamental limits and the ultimate achievable device performance. Also, important specific physical parameters of specific systems can often be computed using this method. Finally, practical device design trade-offs and guidelines for this class of optoelectronic devices can be formulated on the basis of the understanding provided by the investigation of the fundamental physics.

PROGRESS

This task included the following three areas: (1) near band gap femto-second optical probing and carrier relaxation, (2) fundamental physics of operation of optical detectors, (3) fundamental physics of optical sources.

Research in area (1) had been completed. Many non-equilibrium, many-body physical processes, such as Coulomb enhancement, band renormalization, carrier-carrier scattering, and dynamic carrier screening, were found to be important factors in the relaxation of carrier generated using ultra-fast optical pulses. These processes were all included in the formulations and simulation of carrier relaxation. The resulting ensemble Monte Carlo code was used to study carrier relaxation on the time scale from 100 fs to about 2 ps in the near-band-gap excitation regime. Excellent agreement of the simulation results with experimental data was found and explained without using any adjustable parameters [17, 18]. This placed much confidence in the validity and accuracy of our self-consistent semi-classical ensemble Monte Carlo method, which explicitly includes non-equilibrium and many-body phenomena. Details of this work have been reported in JSEP publications.

Based on this understanding of carrier dynamics and optical interactions, we embarked on the study of the fundamental intrinsic operation of metal-semiconductor-metal (MSM) photodetectors on the femto- and picosecond time scales. In order to keep the problem tractable, a one-dimensional real space and three-dimensional momentum space configuration was used. All relevant physical conditions and processes in

photodetectors were incorporated, including inhomogeneous doping, short spatial length scale variations in the carrier density, spontaneous emission, metal-semiconductor contacts, and a conduction band structure with Γ and L valley minima. Holes were of course fully included as well.

An extensive study of the fundamental response and operation of MSM photodetectors has been completed [17]. It was found that the ultra-fast photo-current response (Fig. 1) of these detectors has three components: the initial fast Γ electron overshoot component, the slower secondary electron contribution in the L valley which lies about 320 meV higher than the Γ point in GaAs, and the slowest third component originating from the hole drift current.
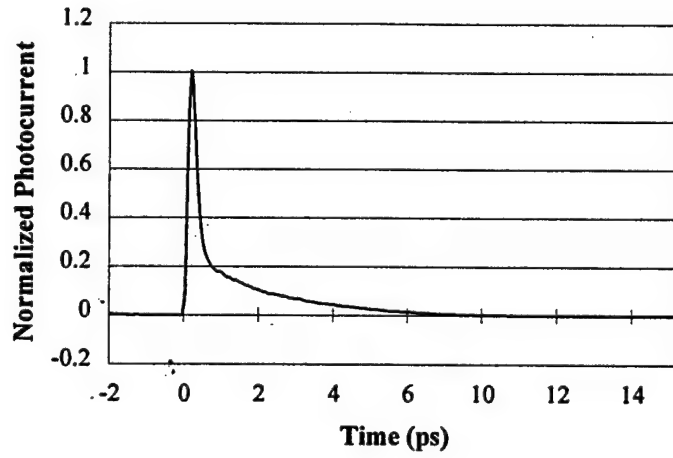

Fig. 1. Fundamental photocurrent response of an MSM photodetector for 0.5 μm device length with a 20 kV/cm applied field (left graph). A femtosecond pulse has generated the electron-hole pairs.
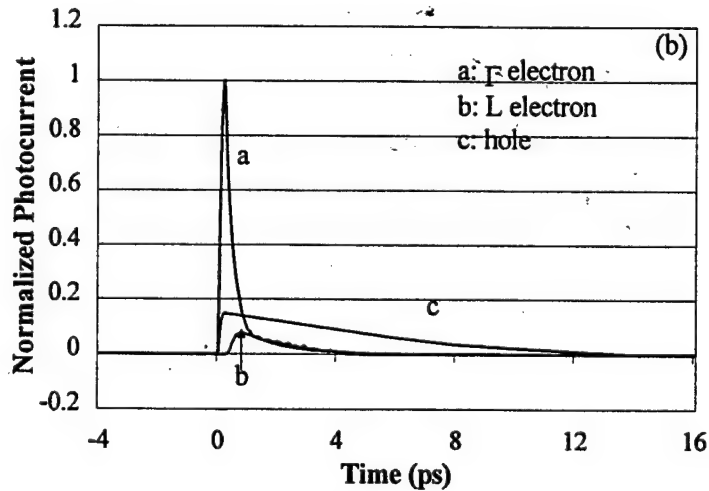

Fig. 2. Contributions of the Γ valley electrons, L valley electrons, and holes, for 0.5 μm device length, 20 kV/cm applied field to the fundamental photocurrent response of an MSM for 0.5 μm device length with a 20 kV/cm applied field (right graph). A femtosecond pulse has generated the electron-hole pairs.

It was further found that each of these components can be significantly affected by external electric fields and by the length of the device in complex ways (Fig. 3, 4). Generally, the transient phase of the response, consisting of fast electrons, is more prominent in cases with lower external electric fields and/or shorter device lengths. The effect of the excitation photon energy on the response of the two electron populations is also significant (Fig. 5). Excitations high above the band edge heat electrons very quickly and cause them to transfer into the slower L valley, thus increasing the electron transit time (Fig. 5). Screening of the electric field by the excited carriers was observed at high excitation levels.

As stated above research in area (3) was de-emphasized and more effort devoted to the understanding and development of the first-principles physical formulation. This effort has provided additional insights into the physics of III-V laser materials and devices via further investigation of carrier generation, relaxation, and transport. Our previously developed formulations and models are of course fully relevance to all optoelectronic devices including lasers.

We found that the scattering rates and energy transfer rates of carriers on the femtosecond scale obtained from our dynamic model are quite different from those obtained from other models (Figs 1, 2). Although these results were obtained under condition of equilibrium, they are relevant to lasers in that they are derived from a dielectric function that is dependent on the ever-evolving distribution functions of the carriers. Modulation of semiconductor lasers involves carrier transport, and the maximum modulation frequency depends on the rate of carrier relaxation. The dynamic model shows the significance of carrier-carrier scattering and dynamic screening in such relaxation processes.
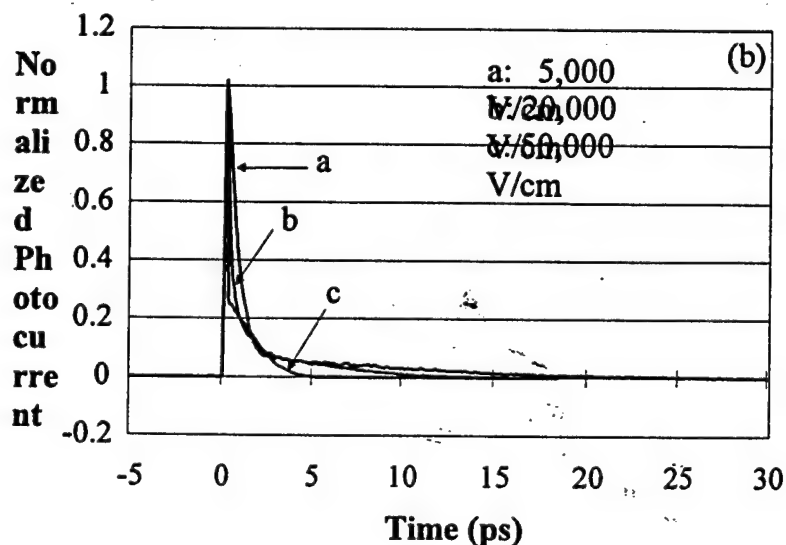

Fig. 3. Normalized photocurrent response of an MSM photodetector with a 0.25 μm device length for three electric fields: 5, 20 and 50 kV/cm (left graph).
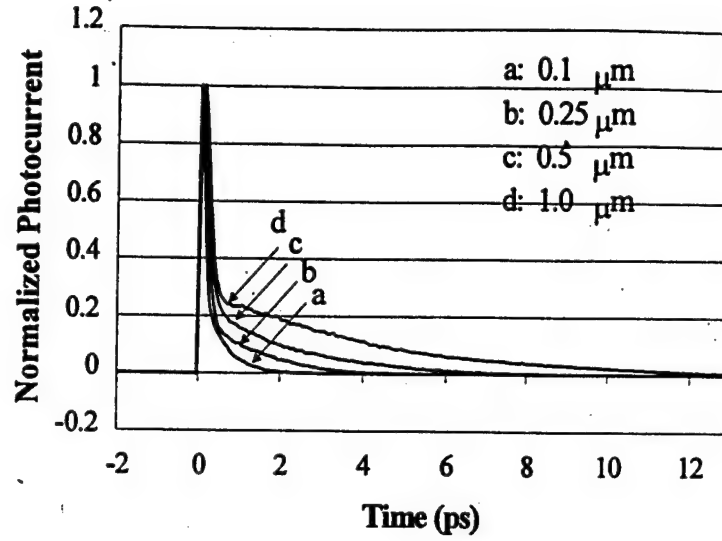
Fig. 4. Normalized photocurrent response of an MSM photodetector with an electric field of 20 kV/cm and four device lengths: 0.1, 0.25, 0.5 and 1.0 μm.
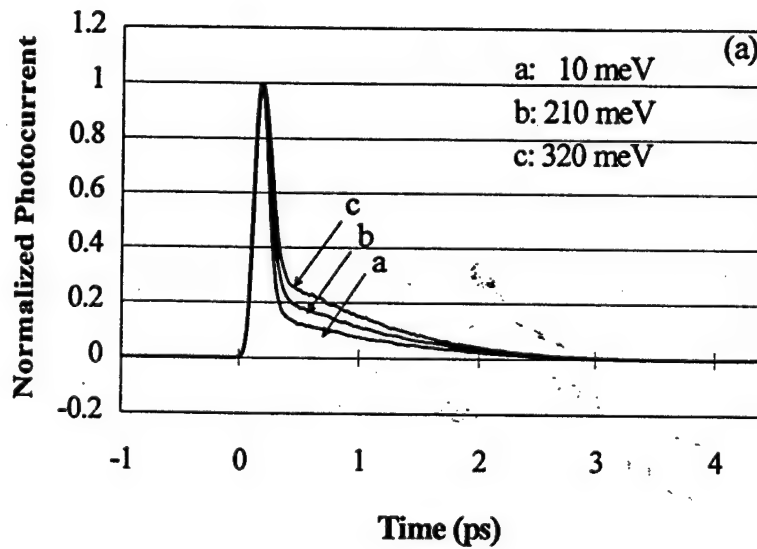

Fig. 5. Normalized photocurrent response on a MSM photodetector with 0.25 μm device length a 40 kV/cm electric field for three photon excitation energies: 10, 210, and 320 meV above the direct gap band edge.
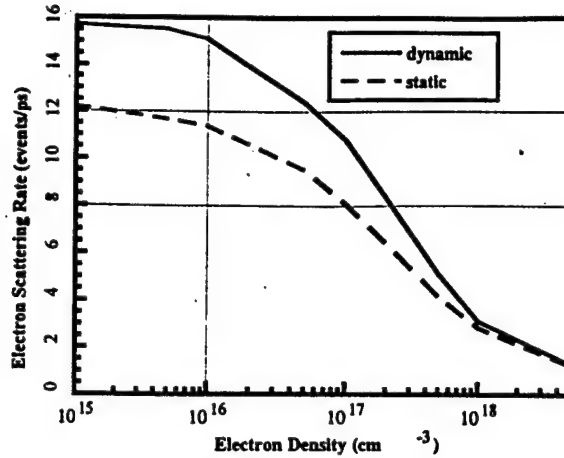
Fig. 6. Average electron-electron scattering rate as a function of electron plasma density as computed from the self-consistent ensemble Monte-Carlo method for dynamic and static screening (left graph). The III-V material is $In_{0.53}Ga_{0.47}As$ and temperature 300K.
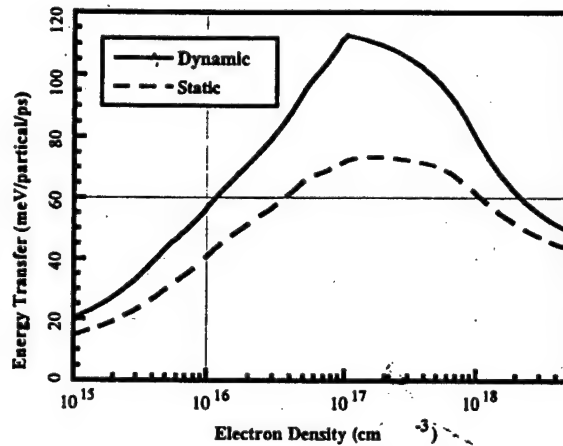

Fig. 7. Average electron-electron energy transfer rate as a function of electron plasma density as computed from the self-consistent ensemble Monte-Carlo method for dynamic and static screening (right graph). The III-V material is $In_{0.53}Ga_{0.47}As$ and temperature 300K.

We have further investigated the impact of the photon excitation energy and the femtosecond optical pulse intensity on the carrier relaxation in compound semiconductors. While it might appear that the effects of the pulse intensity is relevant to lasers, the effects of excitation photon energy are not, because lasers do operate at fixed wavelengths. However, our investigation shows that the effects of pulse intensity and the effects of excitation photon energy are intimately linked to each other through the presence of two many-body processes, Coulomb enhancement and band renormalization. These two processes convert changes in pulse intensity, and hence carrier density, into changes in effective band gap and hence in effective excitation photon energy. These latter changes in turn affect carrier densities and dynamics, making the carrier processes in lasers highly complex. Within our framework, all these effects are treated in a self-consistently and therefore their interaction are fully included.
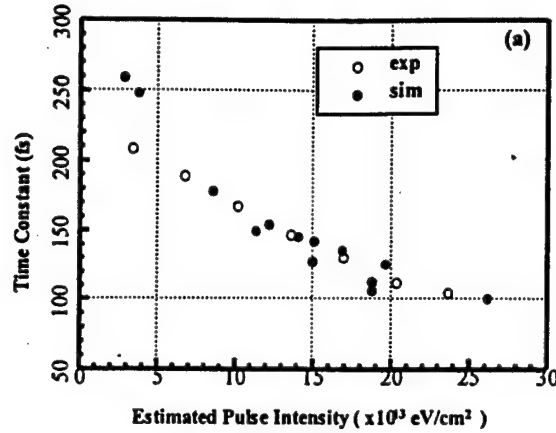
31

Fig. 8. Comparison of exponential time constants obtained from the tails of pulse-probe and actual equal-pulse-correlation experiments as a function of pulse intensity (left graph). Both simulated and measured results are given. The pulse photon energy is 0.806 eV and the band gap is 0.75 eV. The experimental pulse intensities have been multiplied by a factor 1.8 for the purposes of comparison.
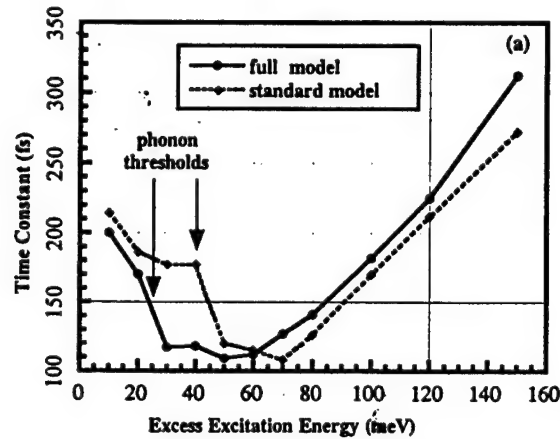

Fig. 9. Comparison of exponential time constants obtained from simulated pulse-probe experiments as a function of photon energy between full model and standard model (right graph). The pulse intensity and pulse width were 3.8×10^{13} eV/cm^2 and 175 fs respectively.

Figs. 8 and 9 illustrate the effects of excitation photon energy and pulse intensity on carrier relaxation. They involve rich physical phenomena [17] that will be present in III-V lasers. These fundamental phenomena can serve as a solid foundation for future research into fundamental carrier dynamics in semiconductor laser device structures.

SCIENTIFIC IMPACT

The investigation femtosecond carrier exitation, relaxation and transport in III-V semiconductor materials using the self-consistent Ensemble Monte Carlo method developed in this work has produced results that are in remarkable agreement with measured data on near band gap carrier relaxation [18]. This lends credibility to the validity and completeness of the present method to described complex non-equilibrium phenomena in optoelectronic devices. The understanding of the interplay between several fundamental carrier processes, including Coulomb enhancement, band renormalization, carrier-carrier scattering, and dynamic screening, has been significantly enhanced. The results and insights gained from this investigation will continue to be highly relevant to and useful for the investigation of the fundamental physics of lasers

based on ultra-fast compound semiconductor materials. Furthermore, the sophisticated, comprehensive simulation methodology that was developed in this task has been shown provide fundamental insight and design guidelines for optoelectronic devices constructed from these materials. As the computational capability of digital computers improves more and more of the physics explored in this task can be exercised in complex practical device structures that operate under highly non-equilibrium conditions in three dimensions.

REFERENCES

1. "Origin of Nonlinear Gain Saturation in Index-Guided Laser Diodes", R. Frankenberger and R. Schimpe, Appl. Phys. Lett., 60, 22, 2720 (1992).

2. "The Gain and Carrier Density in Semiconductor Lasers Under Steady-State and Transient Conditions", B. Zhao, T. R. Chen, and A. Yariv, IEEE J. Quant. Elec., 28, 6, 1479 (1992).

3. "Longitudinal Spatial Instability in Symmetric Semiconductor Lasers due to Spatial Hole Burning", R. Shatz, IEEE J. Quant. Elec., 28, 6, 1443 9 (1992).

4. "Band Gap Shrinkage in GaInAs/GaInAsP/InP Multi-Quantum Well Lasers", S. H. Park, J. I. Shim, K. Kudo, M. Asada, and S. Arai, J. Appl. Phys., 72, 1, 279 (1992).

5. "Effect of Free Carriers on the Linewidth Enhancement Factor of InGaAs/InP (strain layered) Multiple Quantum Well Lasers", L. F. Tiemeijer, P. J. Thijs, J. J. M. Binsma, and T. V. Dongen, Appl. Phys. Lett., 60, 20, 2466 (1992).

6. "Carrier-Induced Change in Index, Gain, and Lifetime for $(InAs)_1/(GaAs)_4$ Superlattice Lasers", N. K. Dutta, N. Chand, and J. Lopata, Appl. Phys. Lett., 61, 1, 7, (1992).

7. "Heterojunction Vertical FET's Revisited: Potential for 225 GHz Large Current Operation", S. Weinzierl and J.P. Krusius, IEEE Transactions on Electron Devices, 39, #5, 1050-1055 (1992).

8. "New Dynamic Model for Multimode Chirp in DFB Semiconductor Lasers", A. J. Lowery, IEE Proc., J137, 5, 293 (1990).

9. "Modelling Spectral Effects of Dynamic Saturation in Semiconductor Laser Amplifiers Using the Transmission-Line Laser Model", A. J. Lowery, IEE Proc., J136, 6, 320 (1989).

10. "Circuit Theory of Laser Diode Modulation and Noise", J. Arnoud, M. Esteban, IEE Proc., J137, 1, 55 (1990).

11. "Two-Dimensional Theory of Distributed Feedback Semiconductor Lasers", H. Sato, and Y. Hori, IEEE J. Quant. Elec., 26, 3, 467 (1990).

12. "Theory of Hot Carrier Effects on Nonlinear Gain in GaAs-GaAlAs Lasers and Amplifiers", B. N. Gomatam and A. P. DeFonzo, 26, 10, 1689 (1990).

13. "Chaos in Semiconductor Lasers with Optical Feedback: Theory and Experiment", J. Mork, B. and Tromborg, J. Mark, IEEE J. Quant. Elec., 28, 1, 93 (1992).

14. "Dynamic Detuning in Actively Mode-Locked Semiconductor Lasers", P. A, Morton, R. J. Helkey, and J. E. Bowers, IEEE J. Quant. Elec., 25, 12, 2621 (1989).

15. "The Effect of Electronic Feedback on Semiconductor Lasers", K. and M. M. Ibrahim, IEEE J. of Quantum Elec, 26, 8, 1347 (1990).

16. "A Self-Consistent Two-Dimensional Model of Quantum-Well Semiconductor Lasers: Optimization of a GRIN-SCH SQW Laser Structure", IEEE J. of Quantum Elec., 28, 4, 792 (1992).

17. "Monte Carlo Simulation of Ultrafast Carrier Dynamics and Optical Interaction in Compound Semiconductor Thin Films and Optical Devices", James E. Bair, Cornell University Ph.D. thesis, pp. 1-359 August 1995.

18. "Femtosecond Relaxation of Carriers Generated by Near-Band-Gap Optical Excitation in Compound Semiconductors", J. E. Bair et al, Phys. Rev. B vol. 50, No. 7, pp. 4355-4370 (1994).

DEGREES AWARDED

Hao Tang, Study of Fundamental Operation of MSM Type Optical Detectors and Carrier Processes in III-V Compound Semiconductors Materials, Master of Science Thesis, submitted to Cornell University, June 1999.

JSEP PUBLICATIONS

1. J.E. Bair, H. Tang, and J.P. Krusius, "Fundametnal MSM Photodetector Response on Femto- and Picosecond Picosecond Scales", submitted to IEEE J. Lightwave Technology, August 1999.

2. J.E. Bair, H. Tang anf J.P. Krusius, "Effects of Excitation Photon Energy and Pulse Intensity on Relaxation of Carriers Excited Near Band Gap in III-V Semiconductors", submitted to Journal of Applied Physics, August 1999.

3. J.E. Bair, H. Tang, and J.P. Krusius, "Monte Carlo Investigation of Dynamic Screening and Carrier-Carrier Scattering on Carrier Transport in Compound Semiconductors", submitted to Journal of Applied Physics, August 1999.

JSEP RELATED PUBLICATIONS

1. J. Sutherland, G. George and J.P. Krusius, "Alignment Tolerance Measurements and Optical Coupling Modeling for Optoelectronic Array Interfaces", Proceedings of the 46th Electronic Components and Technology Conference, IEEE 96CH35931, pp. 480 - 486, 1996.

2. J. Sutherland, G. George, and J.P. Krusius, Modal Optical Coupling Modeling for Multi-Mode Fiber Connections, Manuscript in Progress, to Be Submitted for Publication to IEEE Journal of Lightwave Technology, September 1999.

3. J. Sutherland, R. Johnson, and J. P. Krusius, Modal Optical Coupling Modeling for Laser Diode-to-Multi-Mode Fiber Interconnections, to Be Submitted for Publication to IEEE Journal of Lightwave Technology, September 1999.

Task #5 LONG WAVELENGTH (1.3/1.55 μm) VERTICAL CAVITY LASERS FOR HIG SPEED COMMUNICATIONS

Principal Investigator: Yu-Hwa Lo, (607)255-5077

OBJECTIVE

The objective of the research task is (1) to develop enabling technologies to fabricate 1.3/1.55 μm wavelength vertical cavity surface emitting lasers, (2) to optimize the device performance through understanding of device physics, and (3) to develop viable technologies for VCSEL integration on Si for applications such as optical communication and interconnect.

DISCUSSION OF STATE OF THE ART

Welch et al recently demonstrated 1.3 μm VCSELs that can operate at higher than 80C with greater than 1 mW output power using the wafer bonding technology. However, the devices produce multi spatial modes and are optically pumped by integrated 980 nm GaAs VCSELs. The UCSB group has recently discovered that by introducing superlattices at the p/p InP/GaAs bonding interface, the interface resistance can be reduced and the internal quantum efficiency of the laser is enhanced. As a result, the 1.55 μm VCSELs can achieve 80C CW operation under true current injection conditions. In addition to wafer bonding, people are vigorously exploring other approaches, including N-doped InGaAs, self-assembled quantum dots, and Sb-compounds. At present, none of these alternative approaches have shown device performance close to what have been demonstrated by wafer bonded VCSELs. On the other hand, although the works by Welch and UCSB showed performance improvement of long wavelength VCSELs, their studies also revealed the tremendous technical challenges 1.3/1.55 μm VCSELs are facing. It calls for new device design and enabling processing technologies to turn long wavelength VCSELs into commercially viable devices.

PROGRESS

We are one of the first groups that demonstrated 1.3/1.55 μm VCSELs using direct wafer bonding technology. The basic device structure contains InP-based strain-compensated multi-quantum-wells, a bottom GaAs/AlAs DBR mirror, and a top dielectric mirror, as shown schematically in Figure 1. The device performance critically depends on two factors: the resistance across the GaAs/InP bonding interface and the effectiveness of lateral current confinement. High interface resistance enhances the Ohmic heating effect and raises the junction temperature, considered as the key performance limiting factor. We found that the p-p InP/GaAs fused junction has high resistance and shown a hysteresis loop in its I-V characteristics due to the high density of surface states. Hence an n-n InP/GaAs fused junction is preferred from the point of view of resistance reduction. However, the n-n fused junction imposes two additional problems in device fabrication. First, to achieve an n-n fused junction, the active layers have to have a p-layer down structure where Zn-diffusion into the active layer may be a problem. Secondly, the lateral carrier confinement, the other critical performance limiting factor, becomes more difficult to achieve because of the much higher electron mobility than holes. In other words, electrons can spread farther out laterally than the physically defined laser aperture. The current that bypasses the laser aperture is considered as the leakage current, thus raises the laser threshold. Through device/process optimization using technologies that are currently available to us, we demonstrated 1.3 μm VCSELs with 1 mA threshold currents and the highest operation temperature of 45 C (see Figures 2-3). Although these are the record results for 1.3 μm VCSELs, they are still much inferior to the results demonstrated by GaAs VCSELs and can not meet the specifications for commercial applications. It calls for new device design and enabling processing technologies to turn long wavelength VCSELs into commercially viable devices. This motivates our second phase of research on long wavelength VCSELs, which incorporates several new features into the devices.
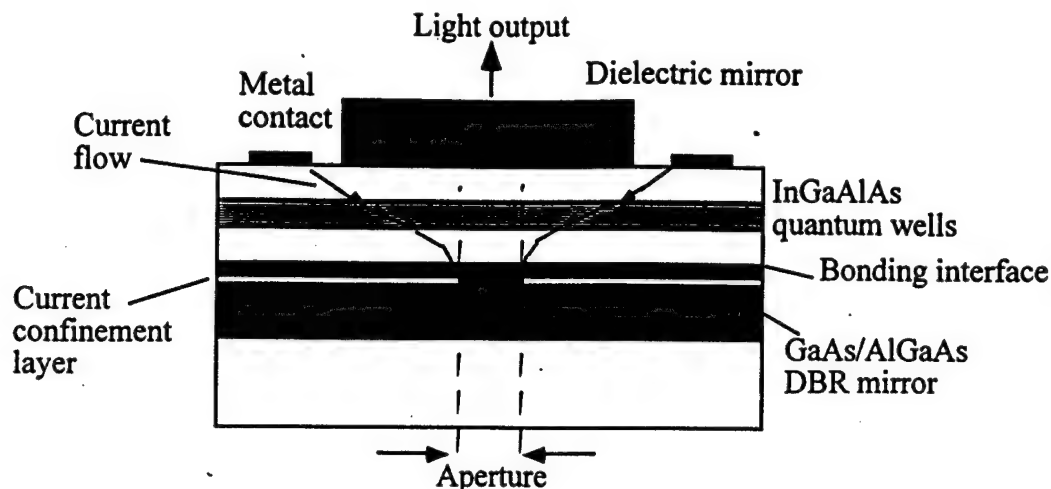
Fig. 1. Schematic of wafer-bonded 1.3 μm VCSEL with an embedded current confinement layer.

(1) Using Esaki junctions and multiple groups of quantum wells

One fundamental difficulty in any long wavelength VCSELs is the high Auger recombination rate and high temperature sensitivity. Although our 1.3 μm VCSELs can operate up to at least 110C (limited by the heating capacity of the TE cooler) in pulsed condition, the devices can only operate at 45C in CW due to Ohmic heating. If one wants to use the multi-layer DBR mirror, the series resistance of the DBR mirror and the Ohmic contact resistance will inevitably increase the total series resistance to a minimum of about 50 Ω, much higher than the typical resistance (6 Ω) for edge-emitting 1.3 μm lasers. Due to the simple I^2R relation for Ohmic heating, one has to reduce the operation current to a minimum and to increase the internal quantum efficiency to greater than 100%! This sounds impossible, but can actually be achieved using Esaki tunnel junctions to connect multiple groups of quantum wells in the laser active region.
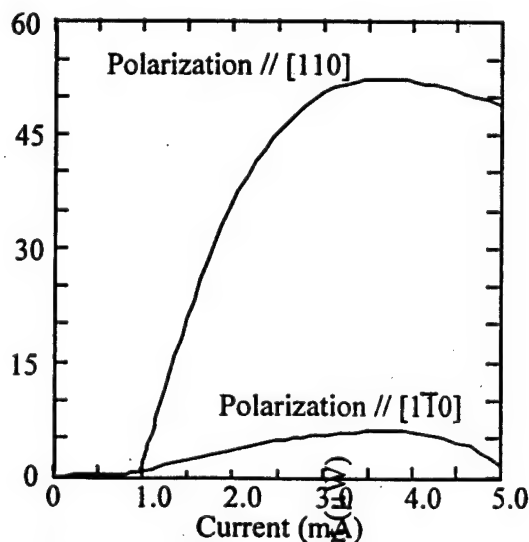

Figure 2. L-I characteristics
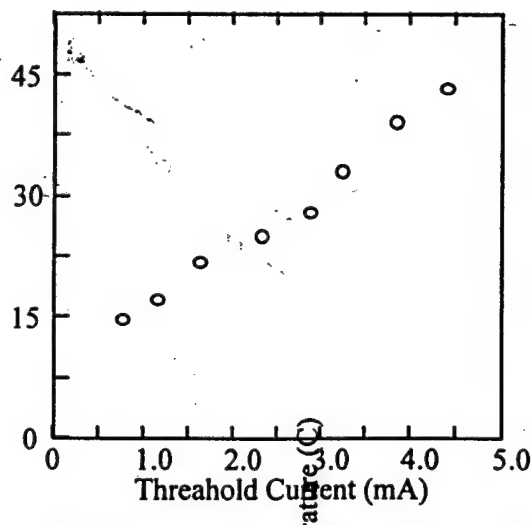
Figure 3. Dependence of threshold current on temperature.

In the ideal case where series resistance is zero or negligible, using a single quantum well group or multiple quantum well groups connected with Esaki junctions is expected to yield similar device performance. The design with Esaki junctions trades current with voltage, so the laser will operate at a higher voltage with a lower current, leading to the same wall plug power efficiency to the first order. However, if the series

resistance becomes significant, as in the case of 1.3/1.55 μm VCSELs, the Esaki junction design will be much more power efficient than the conventional design. Having two quantum well active regions separated by an Esaki junction, the threshold current of the laser is reduced to about half of the original value (with the bias voltage doubled), thus the Ohmic heating is reduced by a factor of 4. Above threshold, one injected carrier will be used twice, once in each quantum well region, to generate twice as many photons and optical gain as the conventional structure, hence the internal quantum efficiency can be greater than 100%. Taking into account all other factors, Figure 4 shows the maximum CW operating temperatures for 1.3 μm VCSELs as a function of the series resistance. Clearly the VCSELs using Esaki junction(s) to connect different groups quantum wells are much less sensitive to the series resistance than conventional VCSELs.

(2) InAlAs Oxidation Layer for Current Confinement

One key reason why GaAs VCSELs work so well is the availability of selectively oxidized AlGaAs. At around 400C in steam, the AlGaAs layer with high Al concentration can be laterally oxidized to form a very stable insulating layer to confine carriers laterally. However, one can not easily find materials having similar properties in InP-based long wavelength VCSELs. Previously, we used the wafer bonded AlGaAs layer for current confinement. Because the distance between the current confinement layer and the quantum wells is separated by several thousand Angstroms, the problem of current spreading still exists, although to a lesser degree. Several research groups including ours have been looking into materials that are compatible with InP and can be selectively oxidized as AlGaAs. Our initial work of lateral oxidation of AlInAs has shown that InAlAs with 48% aluminum may be a good material candidate for current confinement. We have demonstrated a reasonable oxidation rate of the order of 1 μm/min at 450 C and a lateral oxidation layer as deep as 25 μm from the edge of the mesa can be formed out of InAlAs. The electrical and optical property of the oxidized InAlAs is adequate for current and optical confinement. The Auger analysis showed that during oxidation, the In and As atoms leave the material or form precipitates near the oxide/semiconductor interface so the oxide is mostly AlO. However, the relative high oxidation temperature has caused thermal damage to the nearby InP layers. The challenge is to find an effective protection layer lattice matched to InP so that when AlInAs is oxidized, the InP layers are properly protected. Our recent experiment has found that a pair of thin strained InGaAs (30% In) layers that sandwich the InAlAs oxidation layer showed promise for this purpose. With the InAlAs selective oxidation layer and the Esaki junction described previously, we can expect in confidence that 1.3/1.55 μm VCSELs of much improved output power and operating temperature can be achieved.
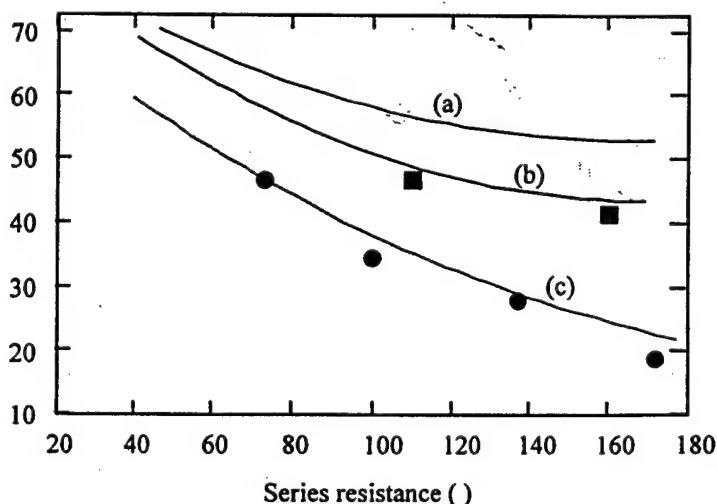

Fig. 4. Maximum CW operation temperature for 1.3 μm VCSELs of different series resistance with (a) three groups of quantum wells connected by 2 Esaki junctions, (b) two groups of quantum wells connected by 1 Esaki junction, and (c) conventional VCSELs. Curve (a) is calculated using a long wavelength VCSEL simulation program without experimental data.

(3) VCSEL Integration on Si

Because one of the ultimate goals for VCSEL research is to achieve optoelectronic integrated circuits for applications such as optical interconnects, we have also expanded our research effort to VCSEL integration on Si. Since long wavelength VCSELs are not mature enough for integration with Si microelectronic circuits, we have used GaAs short wavelength VCSELs for this study. However, the enabling integration technologies developed here can be applied to long wavelength VCSEL integration as well. For integration of III-V with Si, wafer bonding is the prevailing approach due to the high quality material the process produces. However, the wafer bonding process used to make long wavelength VCSELs creates a serious problem for integration of III-V and Si because of the large thermal stress. Among semiconductors, Si has about the lowest thermal expansion coefficients. When compound semiconductors such as GaAs is bonded to Si at high temperature (typically 550 to 700C), the GaAs layer will be under severe tensile stress after the sample is cooled to room temperature. The high built-in tensile stress in GaAs, which is many times of the yield stress, can generate dislocations, cause bedonding, and create film cracking. Therefore, a different wafer bonding process than GaAs/InP bonding has to be developed for VCSEL integration on Si.
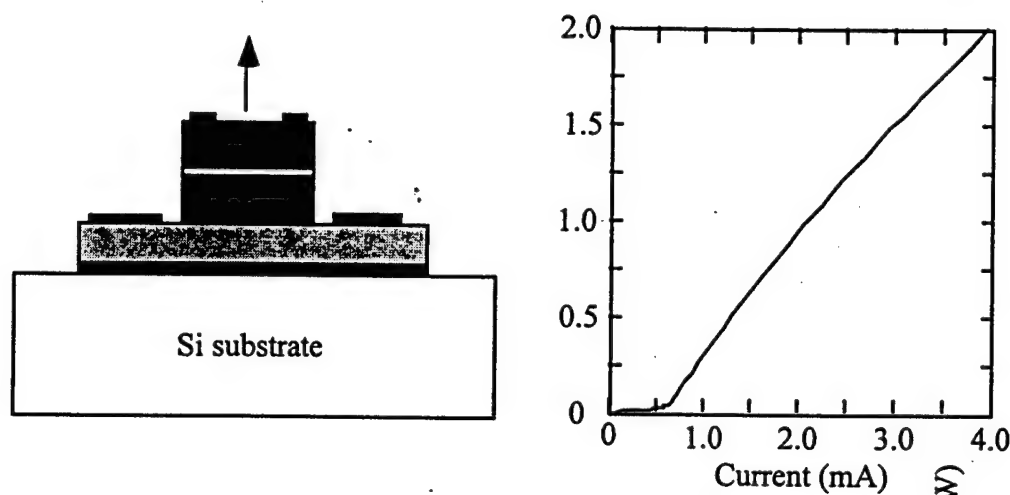

Fig. 5. Schematic and L-I characteristics of GaAs VCSELs on Si substrates.

Over the last year, we have demonstrated, for the first time, a room temperature wafer bonding process that can fuse GaAs epitaxial material directly to Si using spontaneous surface reaction. The bonding strength was found to be at least 50% of the intrinsic Si-Si bond (i.e about 3 Joules/m^2), sufficient for all device processing. Because the GaAs layers were bonded to Si at room temperature, the GaAs devices are stress free during normal operation conditions. Even when the temperature rises for a short period of time for VCSEL process (e.g. 400C Ohmic contact alloying), the GaAs layer is under compression instead of tension so film cracking, a most common problem for GaAs/Si heterogeneous material, does not occur. Figure 5 shows the L-I characteristics of GaAs VCSELs on Si. The threshold current (620 µA), the external quantum efficiency (55%), and the output power (>4 mW) are all the record values for VCSELs on Si.

In summary, although the JSEP research has to end early, we have made significant progress in long wavelength VCSELs and VCSEL integration on Si. In the first design involving wafer bonded DBR mirrors and InP-based quantum wells, we have demonstrated 1.3 µm VCSELs with world record performance in their threshold currents. A cw threshold current of 1 mA and a pulsed threshold current of 0.85 mA were achieved. The results of the first VCSEL design also reveal the problems of high series resistance and ineffective carrier confinement, which leads to the new design of long wavelength VCSELs. The salient features in the new VCSEL design include the use of Esaki junctions to connect different groups of quantum wells in series and selective oxidation of InAlAs for carrier confinement. The concepts and technologies for both approaches have been demonstrated, and research is going on to incorporate both

features into the VCSELs. Finally, studies on the aspect of VCSEL integration on Si were performed. GaAs VCSELs instead of InP VCSELs were used in this study due to the relative maturity of the GaAs VCSEL technology. The key roadblock towards VCSEL-on-Si is the high thermal stress due to the large material thermal mismatch. A room temperature wafer bonding process was then invented to solve the problem and high performance, high yield GaAs VCSEL arrays were demonstrated on Si substrates.

SCIENTIFIC IMPACT

Long wavelength VCSEL is one of the most important optical devices for optical communication. Compared to short wavelength GaAs VCSELs, Long wavelength VCSELs have better eye safety, lower operating voltage, and significantly longer transmission distance and data rate. The bottleneck for the development of long wavelength VCSELs is partly technological and partly fundamental. This research addressed the key technological and scientific issues for long wavelength VCSELs and presented viable solutions to these problems. For example, the problems in mirror reflectivity, current spreading, and ohmic heating can all be solved using the innovative approaches. With further development, it is expected that long wavelength VCSELs will become viable devices for optical communications and interconnects.

DEGREES AWARDED

Alex Tran (Ph. D., 1996): "Optical MEMS technology and applications".
Gina L. Christenson (Ph. D., 1997): "Long wavelength vertical cavity light emitting devices".
Felix E. Ejeckam (Ph. D., 1997): "Theory and technologies of wafer bonding and compliant substrates".
Wan-ning Wu (MENG, 1997): "The search for a compliant universal substrate".
Po Cho (MENG, 1997): "Thermoelectric cooled platform for semiconductor laser characterizing and testing".
Matthew James Springer (MENG, 1997): "An optical power meter".
Min-Te Lee (MENG, 1996): "Preamplifier design in fiber optic transmission".

JSEP PUBLICATIONS

[1] (Invited) Y. Qian, Z.H. Zhu, Y.H. Lo, H.Q. Hou, B.E. Hammons, D.L. Huffaker, D.G. Deppe, W. Lin, M.C. Wang, Y.K. Tu, "Wafer-bonded AlGaInAs 1.3 μm vertical-cavity surface-emitting lasers," *Vertical-Cavity Surface-Emitting Lasers*, SPIE publication, Vol. 3003, pp. 161-168, 1997

[2] (Invited) Z.H. Zhu, F.E. Ejeckam, Y. Qian, J. Zhang, Z. Zhang, G.L. Christenson, Y.H. Lo, "Wafer bonding technology and its applications in optoelectronic devices and materials," *IEEE Selected Topics in Quantum Electronics*, vol. 3, pp. 927-936, 1997

[3] J. Zhang, Y. Qian, Z.H. Zhu, Y.H. Lo, D.L. Huffaker, D.G. Deppe, H.Q. Hou, B.E. Hammons, W. Lin, Y.K. Tu, "Dosage effects on oxygen implanted single-bonded 1.3 μm vertical-cavity surface-emitting lasers," *IEEE LEOS Proceedings*, pap. ThQ5, vol. 2, p. 426, San Francisco, CA, Nov. 10-13, 1997

[4] (Invited) Y.H. Lo, Z.H. Zhu, "Technologies for heterogeneously integrated photonic and optoelectronic circuits," Int. Electrochemical Society Meeting, San Diego, CA, May, 1998

[5] Y. Xiong and Y.-H. Lo, "Current spreading and carrier diffusion in long-wavelength vertical-cavity surface-emitting lasers", IEEE Photon Tech. Lett., vol. 10, no. 9, p1202-1204, Sept. 1998.

[6] Y. C. Zhou, Z. H. Zhu, D. Crouse and Y. H. Lo, "Electrical Properties of wafer-bonded GaAs/Si heterojunctions", Appl. Phys. Lett. 1998, 73, pp. 2337-2339

[7] Z. H. Zhu, Y. C. Zhou, D. Crouse and Y. H. Lo, "Pick-and-place multi-wafer bonding for optoelectronic integration", Electron. Lett. 1998, 34, (12), pp. 1256-1257

[8] (Invited) Y. H. Lo, Z. H. Zhu, R. Zhou, J. Zhang, D. Dagel, L. N. Srivatsa, Y. Zhou, D. Crouse,"Compliant substrate technology for heterogeneous integration", Critical Reviews On Heterogeneous Integration (1998)

[9] (Invited) D. Crouse, Z. H. Zhu, Y. H. Lo, H. Hou, "Pick-and-place multi-wafer bonding of photonic devices on Si," Proceedings of Integrated Photonics Research (IPR) Conference, Victoria Island, Canada, 1998.

[10] (Invited) Y. H. Lo, Z. H. Zhu, D. Crouse, C. Pu, Y. Zhou, J. Zhang, "Photonic integration using wafer bonding technology," International Photonic Conference (IPC) Proceedings, Taipei, Taiwan, 1998.

[11] (Invited) Y. H. Lo, "Heterogeneous integrated optoelectronic and MEMS circuits," US/Korea Joint Workshop on Frontiers of Optoelectronics Technology, Seoul, Korea, 1998.

[12] Y. Xiong and Y.-H. Lo, "Analysis of current spreading in long-wavelength vertical-cavity surface-emitting lasers", Proceedings of CLEO 98, P241-242, May 1998.

[13] D. Crouse, Z. H. Zhu, Y. H. Lo, H. Hou, "Fabrication of photonic devices on Si using pick-and-place multi-wafer technology," LEOS proceedings, p. 87, 1998.

[14] Y. Zhou, Z. H. Zhu, Y. H. Lo, "Electrical characterization of directly-bonded GaAs and Si," LEOS proceedings, p. 91, 1998.

[15] J. Zhang, D. Crouse, Z. H. Zhu, Y. H. Lo, "Improved lateral wet-oxidation of InAlAs," LEOS proceedings, p. 114, 1998.

[16] Z. H. Zhu, R. Zhou, F. E. Ejeckam, Z. Zhang, J. Greenberg, Y. H. Lo, H. Q. Hou, B. E. Hammons, "Growth of InGaAs multi-quantum wells at 1.3 μm wavelength on GaAs compliant substrates," *Appl. Phys. Lett.*, vol. 72, no. 20, pp. 2598-2600, 1998.

[17] R. Zhou, D. Dagel, Y. H. Lo, "Semiconductor thermionic emission coolers using varying current densities," to be published in Applied Physics Letters (in press).

[18] (Invited) Y. Xiong, J. Zhang, Y. H. Lo, "Wafer-bonded 1.3 μm vertical-cavity surface-emitting lasers," Special Issue on Optical Engineering (SPIE), to be published in December, 1998 (in press).

[19] Chuan Pu, Z. H. Zhu, Y. H. Lo, "Surface micromachined polarization beam splitters," *IEEE Photonics Technology Letters*, Vol. 10, no. 7, pp. 988-990, 1998.

[20] Y. Qian, Z. H. Zhu, Y. H. Lo, D. L. Huffaker, D. G. Deppe, H. Q. Hou, B. E. Hammons, W. Lin, Y. K. Tu, "Submilliamp 1.3 μm vertical-cavity surface-emitting lasers with threshold current density < 500A/cm2," *Electron. Lett.*, vol. 33, pp. 1052-1054, 1997.

[21] Y. Qian, Z. H. Zhu, Y. H. Lo, D. L. Huffaker, D. G. Deppe, H. Q. Hou, B. E. Hammons, W. Lin, Y. K. Tu, "Long wavelength (1.3 μm) vertical-cavity surface-emitting lasers with a wafer-bonded mirror and an oxygen-implanted confinement region," *Appl. Phys. Lett.*, vol. 71, pp. 25-27, 1997.

[22] G. L. Christenson, A. T. T. D. Tran, Y. H. Lo, "Long wavelength resonant vertical cavity LED/photodetector with a 75 nm tuning range," *IEEE Photonics Technology Letters,* Vol. 9, no. 6, pp. 725-727, 1997.

[23] Y. Qian, Z. H. Zhu, Y. H. Lo, D. L. Huffaker, D. G. Deppe, H. Q. Hou, B. E. Hammons, W. Lin, Y. K. Tu, "Low threshold proton-implanted 1.3 μm vertical-cavity top-surface-emitting lasers with dielectric and wafer-bonded GaAs/AlAs Bragg mirrors," *IEEE Photonics Technology Letters*, vol. 9, no. 7, 1997.

[24] Y. Qian, Z. H. Zhu, Y. H. Lo, H. Q. Hou, M. C. Wang, W. Lin, "1.3 μm vertical-cavity surface-emitting lasers with double-bonded GaAs-AlAs Bragg mirrors," *IEEE Photonics Technology Letters*, Vol. 9, no. 1, pp. 8-10, 1997.

[25] (Invited) Y. H. Lo, Z.-H. Zhu, Y. Qian, F. E. Ejeckam, G. L. Christenson,"Wafer bong technology and its optoelectronic applications," Optoelectronic Integrated Circuits, SPIE Publication, Vol. 3006, pp. 26-35, 1997.

[26] G. L. Christenson, A. T. T. D. Tran, S. Miller, D. Haronian, Y. H. Lo,"Surface micromachined interferometer-based optical reading technique," *Appl. Phys. Lett.*, Vol. 69, pp. 3324-3326, 1996.

JSEP RELATED PUBLICATIONS

[1] F. E. Ejeckam, Y. H. Lo, S. Subramanian, H. Q. Hou, B. E. Hammons,"A lattice engineered compliant substrate for defect-free heteroepitaxial growth," *Appl. Phys. Lett.*, Vol. 70, no. 10, 1997.

[2] C. H. Lin, Z. H. Zhu, Y. Qian, Y. H. Lo,"Cascade self-induced holography: a new grating fabrication technology for DFB/DBR lasers and WDM laser arrays," *IEEE J. Quantum Electron.*, Vol. 32, pp. 1752-1759, 1996.

[3] F. E. Ejeckam, M. L. Seaford, Y. H. Lo, H. Q. Hou, B. E. Hammons, "Dislocation-free InSb grown on GaAs compliant universal substrates," *Appl. Phys. Lett.*, vol. 71, pp. 776-778, 1997.

[4] J. A. Smart, E. M. Chumbes, L. N. Srivatsa, Y. H. Lo, J. R. Shealy, "Flow modulation epitaxial lateral overgrowth of gallium nitride on masked 6H-silicon carbide and sapphire surfaces," to be published in J. Vacuum Science and Technology (in press).

[5] (Invited) A. T. T. D. Tran, G. L. Christenson, Z.-H. Zhu, Y. H. Lo, "Micromachined micro-optic and opto-electronic devices," Chapter in Handbook on Opto-Electronics, World Scientific, 1997.

[6] C. Pu, Z. H. Zhu, Y. H. Lo, "Surface micro-machined optical coherent detection system with ultra-high sensitivity," to be published in J. Sensors and Actuators A (in press).

[7] (Invited) Y. H. Lo, Z. H. Zhu, R. Zhou, J. Zhang, D. Dagel, L. N. Srivatsa, Y. Zhou, D. Crouse, "Compliant substrate technology for heterogeneous integration," SPIE: Critical Review on Heterogeneous Integration, 1998.

[8] E. J. Mozdy, M. A. Jaspan, Zuhua Zhu, Yu-Hwa Lo, C. R. Pollock, R. Bhat, Minghwei Hong "NaCl:OH color center laser modelocked by a novel bonded saturable Bragg reflector," *Optics Communications*, vol. 151, pp. 62-64, 1998.

[9] C. K. Kuo, C. H. Thang, S. J. Murry, Chih-Hsiang Lin, A. Delany, S. S. Pei, Y. C. Zhou, Z. H. Zhu and Y. H. Lo,"High-Power Type_II Quantum-Well Lasers", Seventeenth North American Molecular Beam Epitaxy Conference, PennState University, Pennsylvania (10/4-7/1998)

[10] C. Pu, Z. Zhu, Y. H. Lo, "Surface Micromachined Polarization Beam Splitting System," 1998 IEEE/LEOS Summer Topical Meetings, Optical MEMS.

[11] C. Pu, Z. Zhu, Y. H. Lo, "Surface Micromachined Optical Coherent Detection System With Ultra-High Sensitivity," Post-deadline paper, 1998 IEEE/LEOS Summer Topical Meetings, Optical MEMS, Monterey, CA, July 20-22, 1998.

[12] C. Pu, Z. Zhu, Y. H. Lo, "Ultra-Sensitive Optical MEMS Vibration And Polarization Sensors Using Self-Homodyne Detection," Post-deadline paper, LEOS'98, 11th Annual Meeting, Orlando, Florida, Dec. 1-4, 1998.

[13] C. Pu, Z. Zhu, Y. H. Lo, "Highly Sensitive Optical Coherent Detection System Using Surface Micromachining Technology," MEMS'99, 12th IEEE International MEMS Conference, Orlando, Florida, Jan. 17-21, 1999.

[14] C. Pu, Z. Zhu, Y. H. Lo, "MEMS optical self-homodyne polarization rotation sensor for non-invasive glucose monitoring," to be presented in Transducers'99, Japan, June, 1999.

[15] (Invited) Y. H. Lo, Z. H. Zhu, "Silicon compliant substrate for high-quality heteroepitaxial growth," Int. Conf. Solid State Devices and Materials (SSDM) Proceedings, pp. 228-229, Hiroshima, Japan, 1998.

[16] (Invited) Y. H. Lo, "Semiconductor compliant substrates with embedded twist boundaries," Material Research Society (MRS) Meetings, Symposium D, Defect Engineering, San Francisco, CA, 1998. (paper will also be published in the book series by MRS.)

[17] (Invited) Y. H. Lo, "heterogeneously integrated circuits and systems using wafer bonding technology," Material Research Society (MRS) Annual Meeting, Boston, MA, 1998

[18] M. L. Seaford, D. H. Tomich, K. G. Eyink, W. V. Lampert, F. E. Ejeckam, Y. H. Lo, "Comparison of MBE grown InSb on CU substrates using different sacrificial layers," Int. Conf. On Compound Semiconductors, pp. 29-32, San Diego, CA, 1998.

[19] C. Pu, Z. Zhu, Y. H. Lo, "Surface micromachined optical polarizers for magneto-optical data storage," SPIE, Vol. 3328, 1998.

[20] Y. H. Lo, "Semiconductor technologies," 1999 Yearbook of Science & Technology, McGraw-Hill.

[21] (Invited) Y. H. Lo, Z. H. Zhu, "Compliant substrates with an embedded twist boundary," to be published in the J. Vacuum Science and Technology (in press).

Task #6 SCHOTTKY FORMATION on GaInP/GaInAs ANDAlInP/GaInAs FOR USE IN LONG WAVELENGTH DETECTORS AND HIGH POWER HEMT'S

Principal Investigator: Richard C. Compton/Warren Wright, (607) 255-1467

OBJECTIVE

The objective for this work has been to use the previously fabricated MSM photodetectors in a new optoelectronic circuit to generate low phase noise millimeter-wave beat frequencies on optical carriers. The simple material requirements of the metal-semiconductor-metal (MSM) detector make it relatively easy to integrate with more complex devices such as heterostructure transistors. However, in spite of its simple structure, the MSM photodiode is capable of extremely high speed performance.

Low phase noise millimeter-wave beat frequencies, or subcarriers, are needed for signal distribution in a variety of communication and radar systems which stand to benefit from the propagation characteristics of optical waveguide. The feeding of phased-array or active antennas, for example, is an application in which the low loss, small size, low weight and the immunity from electromagnetic interference and crosstalk provided by optical fiber should prove valuable. Millimeter-wave communication systems could also benefit from the optical distribution of signals - by delivering the millimeter-wave signal to remote cells from a central location, antenna complexity could be significantly reduced.

Optoelectronic modules invariably incorporate integrated circuits fabricated on a variety of substrate materials (eg, InP, GaAs, Si) to perform various circuit or optoelectronic functions (eg photodetectors, millimeter-wave amplifiers, mixers, if amplifiers). Packaging and interconnection of such units is an important aspect of system design. The objective of the packaging work is to improve the performance of packaging interconnects used in high-speed and high frequency units employed for data processing, optoelectronics and wireless communications. The first task in such an investigation is the identification of features responsible for the packaging insertion loss in going from one module to another such as, for example, step change in transmission line width or height due to the change substrate dielectric constant. The measurement strategy uses transmission line throughs to replace the device being packaged - a necessary requirement for extracting a model of the packaging transition. Preferred models will use linear circuit simulators with equivalent circuit elements. Successful models can be used to predict circuit response for any chips with known s-parameters thereby reducing developmental costs and time.

The current work has been reported in detail in the JSEP Annual Task Reports for the last two years. The present Report will summarize this work.

DISCUSSION OF STATE OF THE ART

Millimeter-wave Subcarrier Generation

Photodetectors for Optical Phase Locked Loops

High speed photodetectors are in demand for lightwave communications, optical computing, sensors, material characterization, and optoelectronic circuits. Photodetectors can be categorized into two groups, photoconductors and photodiodes. In photoconductors, conductivity is increased through the generation of carriers in a semiconductor region located between two ohmic contacts. Photoconductors have been widely used in optoelectronic circuit characterization such as in pump-probe sampling circuits. The response speed of a conventional photoconductor is limited by material properties, namely carrier transit time, carrier lifetime due to recombination, generation, traps, impurities, and carrier diffusion. Noise is a

major problem in photoconductors. The finite dark conductivity of the device generates a randomly fluctuating background Johnson noise current.

Unlike photoconductors, photodiodes have a rectifying junction which considerably reduces the Johnson noise when reverse biased. In photodiodes, light absorption and electron-hole pair generation occur in the depletion region. Shot noise generated in the depletion region of photodiodes is considerably smaller than Johnson noise in photoconductors. Quantum efficiency and response speed of photodiodes are closely related parameters. Optimizing response speed by minimizing electrode separation in photodiodes dictates that the active area be small which makes focusing light into the device difficult. Therefore, a compromise has to be made between fast response times and high quantum efficiency.

The fastest compound semiconductor detectors reported are GaAs Schottky barrier photodiodes[3] and metal-semiconductor-metal (MSM) photo-detectors[4,5]. Schottky barrier photodiodes require multi-level fabrication steps with level-to-level alignment for high speed response.

In contrast, the MSM detector, has a simple, planar horizontal structure, but requires electron beam lithography to achieve the small electrode spacing required for short transit time operation. MSMs have been reported[4] with finger spacings as small as 25 nm and a response time of 0.87 ps on LT GaAs. The low efficiency of MSM photodiodes is due to the shadowing effect of the metal electrodes, reflection at the semiconductor surface and incomplete absorption in the active layer. An anti-reflection coating can be used to reduce the surface reflection. Superlattice structures have been used underneath the absorption layer to enhance the quantum efficiency by reflecting any of the signal which passes completely through the absorbing region back in the device [5].

In an MSM detector, the electrodes form back-to-back Schottky contacts. With an applied voltage, one contact is always reverse biased, and the leakage through this junction (dark current) adversely affects detection sensitivity. Thus dark current is minimized by forming contacts with high Schottky barriers. On GaAs this is readily accomplished. However, with long wavelength (1.3 μm-1.55 μm) detectors using $In_{0.53}Ga_{0.47}As$ absorbing regions a problem arises due to the low barrier heights on this material. High barriers must be obtained by adding a barrier enhancement layer. A number of different materials have been used for this purpose including $In_{0.52}Al_{0.48}As$ [7] and InP [8], and more recently strained AlInP [9] and GaInP [10]. The latter obtained very low dark current densities of 4.5 pA/μm^2.

To date, the fastest MSMs operating at the longer wavelengths have been achieved with short lifetime material. Impulse responses approaching 1 ps have been achieved with low-temperature grown GaInAs [13], and an GaInAs/GaAs on GaAs super lattice produced a lifetime-limited response of 3.3 ps [14]. Devices fabricated on long-lifetime material have been reported with responses of 13 ps [15] and 14.7 ps [16], though it should be noted that both these values are possibly influenced by measurement system limitations. The spacing between electrodes for these was 1 μm and 1.4 μm respectively; very little work has been done with sub-micron electrode spacing for long wavelength detectors.

Generation of Millimeter-wave Modulated Optical Signals

Numerous approaches have been considered to generate low phase noise microwave and millimeter-wave modulated optical signals. Direct modulation of a diode laser or external modulation is the most straight-forward approach but becomes difficult above 30--40 GHz due to device limitations. Variations on direct laser modulation have been demonstrated which rely on special laser design to facilitate high-frequency modulation. An example is resonantly enhanced modulation, which exploits narrowband peaks in the modulation response at the cavity roundtrip frequency and multiples thereof. This has been achieved with both external cavities [17] and monolithic structures [18], and allows modulation at frequencies above the laser relaxation resonance. Dual-mode lasers have also been used in which the lasers are designed to operate in two modes simultaneously. A distributed feedback (DFB) laser which oscillated on both sides of the Bragg frequency was locked to an externally applied subharmonic of the beat frequency [19; a similar approach was reported in [20].

A second approach to generating millimeter-wave subcarriers is to combine the beams from lasers at slightly different wavelengths. This heterodyne approach is most often carried out by phase locking the beat signal to a stable RF reference source. Such optical phase-locked loops (OPLLs) have been constructed using Nd:YAG lasers [21] and semiconductor lasers. The latter have the advantage of low size and cost, but have the disadvantage of large linewidths which makes necessary large loop bandwidths. For this reason semiconductor lasers have been used with optical feedback to lower the linewidth. This typically entails putting an anti-reflection coating on one laser diode facet and reflecting or diffracting light back into the diode. The first effort to lock semiconductor lasers used this approach [22]. Several other OPLLs using a variety of external cavity configurations have been reported [23-26]. Locking of solitary laser diodes has been achieved by employing loop bandwidths in the 100-200 MHz range [27-29]. The best results were obtained in [29], which were achieved with a 180 MHz loop bandwidth and multi-electrode DFB lasers. Phase variances of 0.02 rad^2 have been achieved for external cavity lasers, and 0.04 rad^2 for solitary lasers. In addition to phase-locked loops, a feedforward technique has also been used to eliminate phase noise in the beat signal of two DFB lasers [30].

In the OPLL results cited above, the largest attainable beat frequency is limited by the frequency of the RF reference source, and good loop performance requires that the loop components (photodetector, amplifier, phase detector) operate at this frequency as well. This report describes a method to overcome this limitation by locking together a series of more than two lasers.

Packaging and Interconnection Issues

Packaging Industry

The packaging of microelectronic silicon chips in a high-speed device might seem only incidental to a machine's design and has no bearing on the overall performance of the system. The facts are otherwise. In many high-speed/high frequency data processing/wireless communication units packaging technology is the factor that determines or limits performance, cost and reliability.

One reason packaging has become so important is the chip-to-chip delay that limits the maximum operating frequency. In order to reduce the delay the chips must be put closer together, resulting in higher crosstalk as switching speed is increased. Meanwhile, a dense array of chips gives off a fair amount of heat, which must be removed efficiently for the circuit to operate properly.

Packaging is an art based on the science of establishing interconnections ranging from zero-level packages (chip-level connections), first-level packages (either single-chip or multichip modules), second-level packages (printed circuit boards), and third-level packages (mother boards).

The most common methods of zero-level interconnects are wire bonding, Tape Automated Bonding (TAB), and solder bumping. Some examples of first-level packages are: Tape carrier Package (TCP), Plastic Quad Flat Pack (PQFP), Ceramic Quad Flat Pack (CQFP), Plastic Leaded Chip Carrier (PLCC), Leadless Ceramic Chip Carrier (LCCC), Plastic Pin Grid Array (PPGA),ceramic Pin Grid Array (PGA), Plastic Ball Grid Array (PBGA), Ceramic Ball Grid Array (CBGA), Small Outline Integrated Circuit (SOIC), Dual In-Line Package (DIP).

In this work, we have focused on the evaluation of zero and first level packaging techniques, specifically wire bonding and LCCC.

In terms of materials, there are two major categories: hermetic and plastic. A hermetic package is constructed of metal and ceramic materials and has a sealed cavity where the chip resides while polymer and metal are the flesh and bones of a plastic package. In general, plastic package is more cost effective than its hermetic counterpart while ceramic package offers more protection against moisture.

Commercial Package Solutions

Thin film, thick film and co-fired are the three basic ceramic processing technologies. They employ different dielectric materials and hence require different processing procedures.

Thin Film MultiLayer: The dielectric in a thin film multilayer is polyimide. Polyimide has the lowest value of dielectric constant (lowest propagation delay) and a low dissipation factor over a wide frequency range. Furthermore, it is chemically inert, very pure, and thermally stable up to 400°C. The good heat resistance enables the polyimide to be operated under general conditions of wire bonding, die bonding, sealing, etc. The maximum thickness of polyimide formed at one operation is about 20 μm (0.008"). Via holes are formed by wet photolithography and the minimum size is about three times the thickness of the polyimide. Both copper and aluminum can be used as a conductor. The metals are ion-plated by the use of electron beam deposition in order to enhance the conductor adhesion. Chromium, whose thickness is less than 100 nm, is used as the substrate metal. The adhesion strength is about 2 kg/mm^2 (2850 psi). The sheet resistance of the deposited thin film copper is observed to have values that are 1.6 times the theoretical value.

Thick Film Multilayer: Conventional thick film systems may use various metals such as gold, silver-palladium, and copper. Copper conductor and glass dielectric are fired at approximately 900°C under a pure nitrogen atmosphere. The sintered conductor has a sheet resistance of approximately 2 Ω/sq at 20 μm (0.0008") thickness. The metalization patterns are produced by screening, producing a coarser pattern than that can be generated by either thin film or co-fired technology. On the other hand, the thick film system has a high dimensional tolerance and geometrical precision very similar to the thin film system.

Cofired Multilayer: Multilayer ceramics (MLC) are monolithic structures of personalized and interconnected ceramic and metal layers. The individual layers can vary from less than one mil to over twenty mils. The materials in greatest use today are titanate dielectrics with palladium metal electrodes for MLC capacitors and a variety of alumina ceramics with either molybdenum or tungsten conductors for MLC substrates. Conventional MLC use a "silk screen" printing method for the formation of traces. Consequently, the MLC cannot meet the requirements for the formation of fine patterns. Minimum line width is about 0.004". Therefore renders it unsuitable for VLSI packages with more than 200 I/O s. Furthermore, the difficulty in using co-fired technology is aggravated by the large dimensional tolerance created by the large shrinkage which occurs during sintering. Low-temperature co-fired ceramic systems offer the benefits of existing thick film technology combined with the processing advantages of co-fired ceramics. They allow cost-effective production of high density multilayer interconnect hybrids with the benefits of in-house control. Low temperature systems developed for in house use are based on glass filled composites, crystallizable glasses and crystalline phase ceramics. The material system consists of a cast green dielectric tape, compatible signal line and via fill conductor compositions, thick film resistor compositions for post- and co-firing on top layers, developmental resistors for buried configurations and thick film conductor compositions for customizing top layers. The material system was designed for compatibility with standard thick film equipment and processing. Thick film printers, drying ovens and belt furnaces can be used in circuit fabrication and additional equipment (laminating presses and via punching devices) is commercially available. Blanking and registration tooling can be readily built.

PROGRESS

Millimeter-Wave Subcarrier Generation

Figure 1 shows the circuit for a standard OPLL. The beams from two lasers are combined and mixed on a photodiode. The beat signal is then mixed with an RF reference for phase detection, and the resulting error signal is filtered and fed back to the bias of one of the lasers. This laser acts as a current controlled oscillator (CCO) and replaces the voltage controlled oscillator normally found in phase-locked loops.
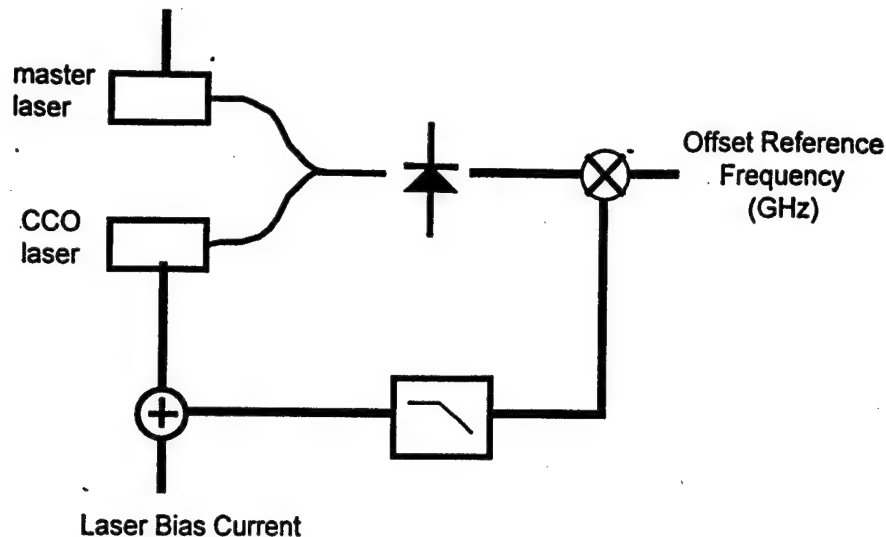
Fig. 1. A heterodyne, or offset, optical phase-locked loop (OPLL). The wideband loop locks the beat signal of the two lasers to a low phase noise reference source.

If a series of many lasers are offset-locked as shown schematically in Figure 2, then essentially arbitrarily large beat fequencies may be obtained. For example, a series of four lasers, each locked 60 GHz higher in frequency than the previous one, can produce a beat frequency of 180 GHz if the first and last beams are combined. In addition, 60 and 120 GHz beat notes are available. In principle all of the signals could be widely tunable.
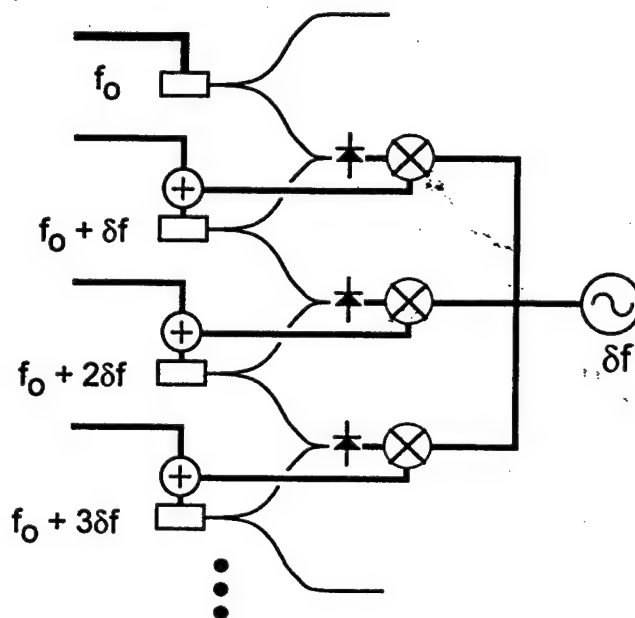

Fig. 2. A series of lasers, each phase-locked to the preceding one with frequency offset δf. Combining the beams of the first and nth produces a beat frequency equal to $(n-1)\delta f$.

This report presents results demonstrating the locking of a series of lasers as described above to generate 33-40.5 GHz beat signals. First, a brief description will be given of the construction and characterization of the narrow linewidth external cavity lasers used in the OPLLs. Secondly, the phase noise for a series of locked oscillators will be analyzed to see what effects such a circuit has on the phase of the resulting beat

47

signals, and lastly, experimental results will be given for 3-laser OPLLs used to generate very low noise (phase variances of 10^{-4} rad^2) subcarriers at 33-40.5 GHz. These results represent a significant improvement over previously reported values for semiconductor lasers [24,29]; roughly two orders of magnitude lower phase variance and a factor of two increase in the beat frequency.

Laser Selection

The critical performance characteristics desired for semiconductor lasers used in OPLLs are 1) single longitudinal mode, 2) narrow linewidth, and 3) suitable FM response. Other qualities such as the ability to be fabricated in an optoelectronic integrated circuit are also desirable and may be beneficial to OPLL performance.

The last requirment for the laser, a suitable FM response, is potentially the most problematic. The FM response is the complex transfer function which relates the laser frequency to bias current modulation. Two effects contribute to the FM response of a typical laser diode: a thermal effect and a ``carrier effect" [31]. The former causes a change in refractive index due to heating, and this leads to a red-shift of the longitudinal cavity modes. The latter results from a refractive index change caused by a change in free-carrier density, and produces a blue shift. The thermal effect dominates at lower modulation frequencies and diminishes at higher frequencies, with the result that the FM response undergoes a phase change of π radians. This ``crossover" point is generally in the low (<10) MHz regime.

The magnitude of the FM response should be large since this will contribute to the loop gain and thus decrease the amount of gain needed elsewhere in the loop. A large magnitude is thus only necessary when it is impractical to compensate with other forms of gain.

The phase of the FM response is a more critical parameter since it contributes directly to the phase of the open-loop gain and reduces the phase and gain margins for the loop. As the phase and gain margins decrease the loop begins to amplify the phase noise of the beat signal at frequencies where the gain is near unity, and at the point of zero margin the loop will oscillate.

From the above considerations two candidate semiconductor lasers appear for use in OPLLs: external cavity lasers and multi-electrode lasers. The latter, while offering the advantage of potential integration into optoelectronic circuits, are currently expensive ($7000) and not widely available. External cavity lasers thus were chosen to demonstrate the concept of phase locking multiple lasers to generate millimeter waves.

Laser Design

The lasers used in the OPLLs must all operate at essentially identical wavelengths and be tunable over a wavelength range sufficient to generate the desired millimeter-wave beat frequencies. This tuning range is small (a fraction of a nanometer) and thus the tuning requirement is significantly relaxed compared to that normally desired from an external cavity laser. As described below, this makes possible the use of commercially available, inexpensive laser diodes such as those used for reading optical disks.

External cavity lasers are typically formed with a laser diode which has one facet antireflection (AR) coated, a collimating lens, and a frequency selective reflector such as a grating. The cavity configuration chosen for this work was the Littman-Metcalf, or grazing incidence, cavity. The lasers used in this work were Sharp LT024-MD. They operate at 785 nm, are capable of 30 mW output power, and have an output facet which is coated to produce a reflection of about 5\% and a rear facet which is coated for high reflection. An 8 mm, 0.5 NA aspheric lens was used for collimation, and a 1800 l/mm, holographic grating was used along with a dielectric mirror. The mirror was mounted on a standard 2-inch optical mount which was modified by the inclusion of a piezo-electric transducer (PZT) to permit electronic control of the cavity length. The cavity length was nominally 10 cm.

Laser Characterization

Characterization of the laser's linewidth and FM response is crucial to ensure proper function of the phase-locked loop. Measurement of the linewidth was performed using a self-heterodyne configuration, [34,35] and the same configuration was also employed to measure both the magnitude and phase of the FM response. To the best of our knowledge this is the first use of a self-heterodyne technique to characterize the FM response of a laser; it has previously been characterized using an FM to AM conversion in the optical domain and network analysis techniques to determine both magnitude and phase of the response [36].

An example self-heterodyne spectrum for a modulated laser is shown in Figure 3 where the spectrum extends to just over 12 MHz. This measurement was made at a modulation frequency of 120 kHz with an amplitude of 200 µA peak-to-peak, corresponding to an FM response of 60 MHz/mA. This particular measurement was made on a DFB laser with external feedback. The external cavity lasers constructed from Sharp diodes had a lower-magnitude FM response of ~4 MHz/mA.
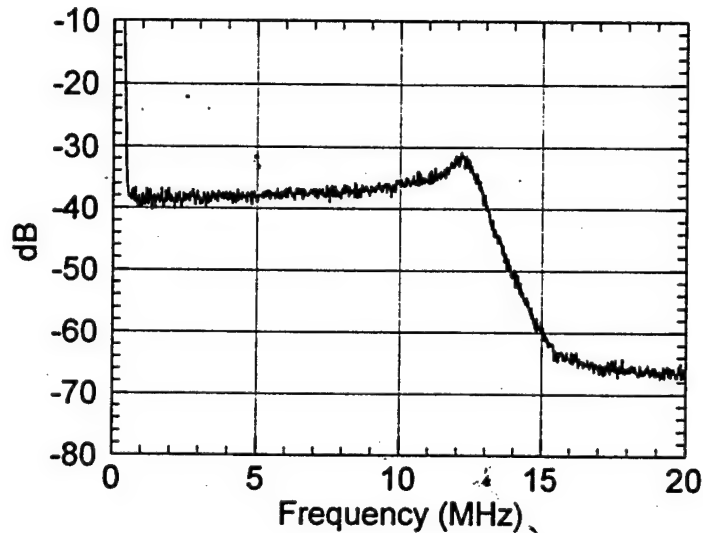

Fig. 3. Self-heterodyne spectrum of a DFB laser with external feedback modulated by a 120 kHz, 200 µA pk-pk sine wave demonstrating a 60 MHz/mA FM response.

Fig. 4 shows the FM response of an external cavity laser constructed with the Sharp laser diodes and measured using the self-heterodyne techniques described above. The magnitude shows an increase at lower frequencies, probably caused by increased thermal effects, while the phase demonstrates a fairly flat response to 2 MHz. The features present in the phase response are likely a result of measurement error, since precise determination of the point f_{inst}=0 is difficult, especially at higher modulation frequencies. Based on this phase measurement, it appears that OPLL loop bandwidths in excess of 2 MHz should be possible since the phase at this frequency is well above $\pi/2$.

The results for linewidth and FM response indicate that the lasers are well suited for use in an OPLL. The combined linewidth is <60 kHz and the highest loop bandwidth obtainable is in excess of 2 MHz, and thus the previous mentioned target values are met.
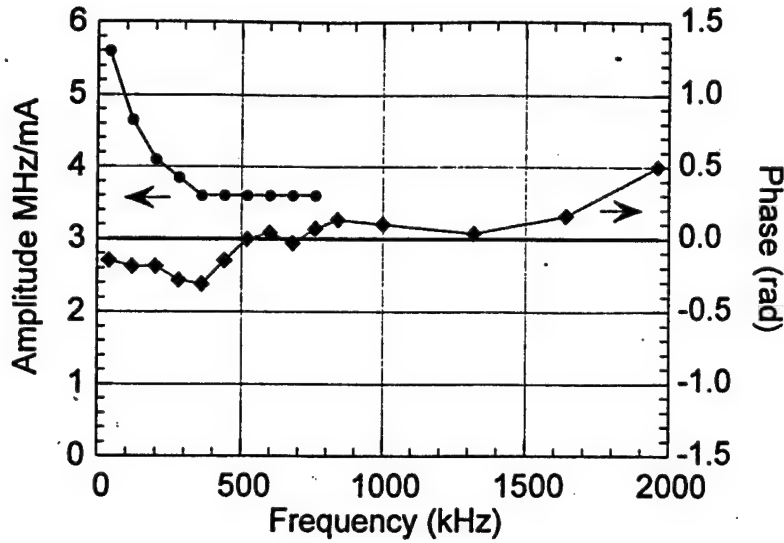
Fig. 4. Magnitude and phase of the FM response of an external cavity laser measured with self-heterodyne techniques.

Phase Noise of Multiple Locked Lasers

In this section, the phase noise of lasers locked in series will be evaluated. It is found that at frequencies where the magnitude of the open-loop gain is near unity, the presence of the open-loop phase serves to amplify the phase noise leading to increasing noise with increasing number of lasers locked. The two possible ways in which three lasers may be locked together are examined and it is found that one configuration results in less noise than the other, a result which is consistent with the experimental results.

In the following, laser i will be modeled as a noise free oscillator with a noise source $\phi_{in}(t)$ added to its phase. Although such a noise source does not have a Fourier transform, for purposes of analysis, $\phi_{in}(\omega)$ will be treated as such. Similarly, the noise of the RF offset reference is taken as $\phi_m(\omega)$. Then the noise of laser i while locked to laser j will be denoted $\phi_i(\omega)$, and is given by

$$\phi_i = \frac{G_{ij}}{1+G_{ij}}\phi_j + \frac{1}{1+G_{ij}}\phi_{in} - \frac{G_{ij}}{1+G_{ij}}\phi_m \tag{1}$$

where $G_{ij}(\omega)$ is the open-loop gain, and for the single free-running (master) laser k, $\phi_k = \phi_{kn}$. For n lasers locked, (1) represents $n-1$ equations which are solved to find the phase of all but laser k as a function of the gains and the noise sources. Generally, the phase of the i th laser will depend on the noise sources of lasers k through i, inclusive.

When locking three lasers together to generate a beat frequency equal to twice that of the shared RF reference there are two possible configurations. If an arrow points from slave to master, then these may be represented as:

Frequency: $f - \Delta \quad f \quad f + \Delta$

Configuration A: $\quad 1 \leftarrow 2 \leftarrow 3$

Configuration B: $\quad 1 \rightarrow 2 \leftarrow 3$.

These two configurations yield somewhat different results. Solving equations (1) and evaluating the beat signal noise $\phi_3 - \phi_{1n}$ of configuration A and $\phi_3 - \phi_1$ of configuration B leads to two conclusions: For both configurations the large-gain limits are the same and yield a phase noise equal to twice that of the reference source. This is the same noise which would be produced by frequency doubling the reference. For gains of order unity it is found that configuration A produces more noise than configuration B. As an example, if $G_{12} = G_{23} = 1$ and the lasers are assumed identical, then, remembering that the laser noise sources are not coherent and ignoring the reference source noise, configuration A will produce 2.4 dB more noise power. This difference will vary depending on the magnitude and phase of the gains, and for practical loops with significant open-loop phase, it could be substantially more. The larger noise of configuration A can be explained intuitively: in the region of $|G| = 1$ the loops increase ϕ_3 by adding contributions from both lasers 1 and 2. The resulting beat noise $\phi_3 - \phi_{1n}$ is increased. In configuration B, the noise of both lasers 1 and 3 are increased with contributions from laser 2, but these contributions cancel when $\phi_3 - \phi_1$ is considered.

Using estimates for the open-loop gain and Lorentzian laser line-width based loosely on the experiments presented in the next section, calculations were made of the total phase variance versus a scaling factor K of the open-loop gain. The results are shown in Figure 8, where it is evident that configuration A produces lower phase noise, less than half that of configuration B. Also, configuration A has a broader minimum which facilitates loop design.
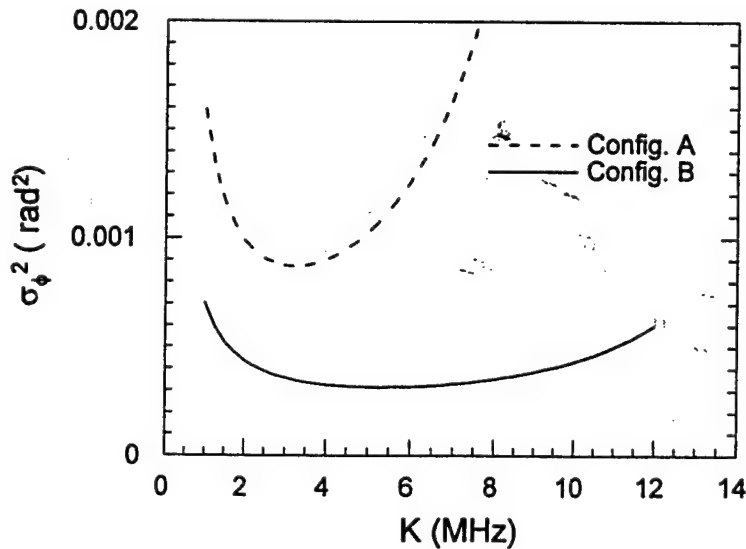

Fig. 5. Phase variance of the beat signal between the first and third lasers for configurations A and B. K is a scaling factor for the loop gain.

Experimental Demonstration

To demonstrate the locking of three lasers in both configurations A and B, three external cavity lasers were constructed as described above. The lasers were operated without any temperature stabilization, though

piezoelectric control of the retro-reflecting mirror was used to help track thermal drift. This control was incorporated into the loop with a low-pass filter. Stable phase locking for periods up to one hour were observed with this arrangement.

To lock three lasers in the fashion depicted in Figure 2 and to monitor the three beat signals would require a large number of microwave and optical components. A simpler solution is to combine all three beams on a single photodiode. Figure 6 shows the experimental arrangement. In this scheme the frequency offsets between the lasers differ by ~500 MHz, allowing diplexing of the DC and 500 MHz signals after the initial down conversion, followed by a subsequent down conversion of the 500 MHz signal. Error signals for each beat signal are thus separated and fed back to the appropriate laser. With this approach all the high-frequency RF components are shared between the two loops and three beat signals, and optical alignment is greatly simplified. Also, the three lasers can be locked in either configuration A or B without changing the hardware configuration.

A disadvantage of combining all beams on a single photodiode is cross talk between the loops as a result of two-tone, third-order intermodulation in the amplifier and mixer. This will cause the error signal from one loop to be introduced into the other. This can be minimized by keeping the power into the amplifier and mixer low. Also, the single-photodiode circuit requires an additional 500 MHz source, and the conversion loss of the second mixer must be compensated for in the loop gain. The latter is easily accomplished.

The circuit using a single photodiode was used to lock three lasers together. An 18-40 GHz amplifier was used (with usable gain below 18 GHz) along with an offset reference with a maximum frequency of 20 GHz, permitting generation of beat signals from ~33 to 40.5 GHz. A 1-μm spacing, GaAs MSM photodiode fabricated earlier in this project was used for the photodetector. Modeling which took into account an estimated laser FM repsonse showed that a flat loop filter (no filter) would result in the lowest phase noise. An active filter with transfer function $(1 + j\omega\tau_2) / j\omega\tau_1$ was used, however, with a large

value of τ_2 to provide a flat response over most of the loop bandwidth but to enhance the gain at lower frequencies where drift, $1 / f$ noise, and mechanical vibration are present. The quantity τ_2 / τ_1 was experimentally adjusted to find the phase noise minimum shown in Figure 5. This resulted in loop bandwidths (frequency at which $|G| = 1$) of ~4 MHz. Loop oscillation ocurred near 8 MHz, presumably caused by the phase of the laser FM response reaching $\pi/2$.
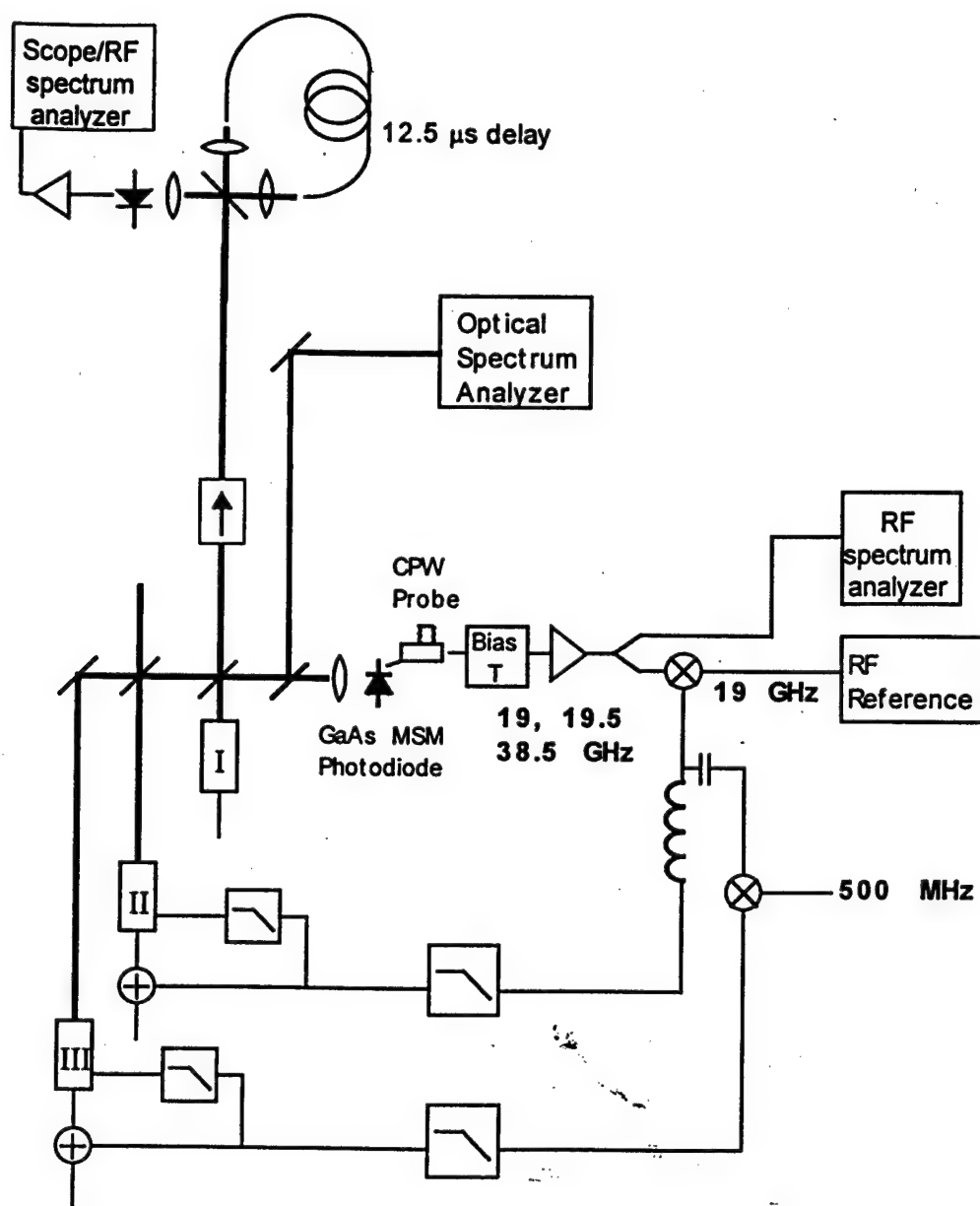
Fig. 6. Experimental setup to phase lock three lasers and generate 33-40.5 GHz beat signals.
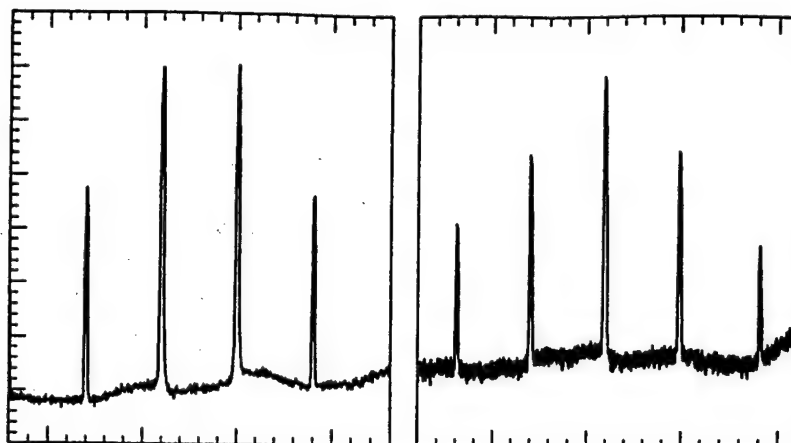
Fig. 7 Signals received from the single photodiode by the spectrum analyzer. The heterodyne signals from the three lasers are at 18.1, 18.5, and 36.6 GHz. The other signals result from inter-modulation in the amplifier.
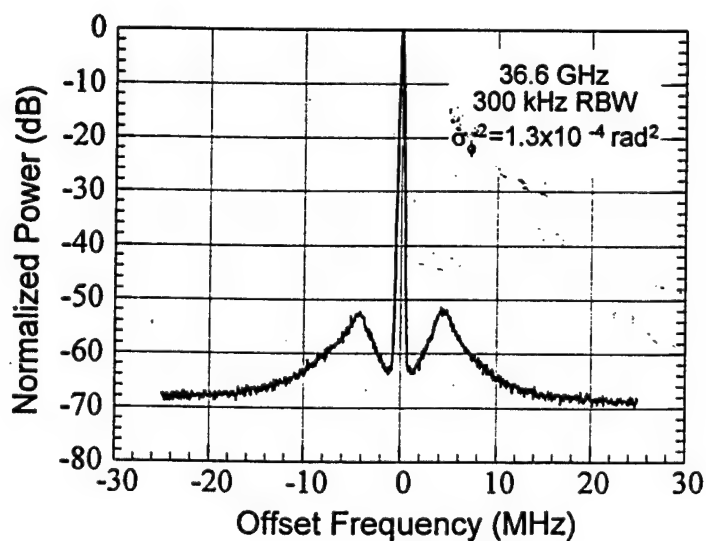

Fig. 8. Narrow-span measurement of the 36.6 GHz signal.

Results for configuration B with beat signals of 18.1, 18.5, and 36.6 GHz are shown in Figures 7 and 8. Figure 7 shows the spectrum analyzer output of the three beat signals along with inter-modulation products generated in the amplifier, and Figure 8 shows a narrow-span spectrum of the 36.6 GHz signal. From the latter curve it is estimated that the total phase variance is $\sigma_\phi{}^2 = 1.3 \times 10^{-4}$ rad^2.

Configuration A produced a variance of $\sigma_\phi^2 = 6.8 \times 10^{-4}$ rad^2, five times that of configuration B. This difference may be attributed in part to the greater noise of configuration A compared to configuration B as discussed above. A second possible cause is a difference in laser line-widths between the two measurements. The lasers' line-widths depend on their tuning with respect to the solitary laser modes [33], and this relation was not controlled experimentally.

The results presented here demonstrate the idea of offset phase locking multiple lasers to generate millimeter wave beat signals. Very low phase noise 33--40.5 GHz sub-carriers have been created by offset-locking 3 external cavity semiconductor lasers constructed from commercial laser diodes. The RF frequency attained is about twice that previously reported for semiconductor lasers, and the low variance σ_ϕ^2 achieved of ~10^{-4} rad^2 is roughly two orders of magnitude lower than previously obtained with semiconductor lasers. The low phase noise is attributed to the narrow laser line-width and the relatively high frequency (~8 MHz) at which the phase of the FM response reached $\pi/2$. Optimizing the loop bandwidth allowed these favorable characteristics to be exploited. With multi-laser phase-locked loops, low phase noise sub-carriers well above 100 GHz should be attainable.

Characterization of Commercial Packaging Modules

The electrical properties of two commercially available microwave hermetic packages were measured using a Wiltron Universal Test Fixture and a Cascade Coplanar Microprobe. Four microwave CAD design tools were used to study and extrapolate the package behaviors. Touchstone was found to give the most accurate representation of the packages through equivalent circuit models.

1. Sonnet A suite of electromangnetic simulation tools capable of drawing, analyzing and visualizing the results of 3-D structures embedded in multilayer dielectrics up to the THz range. It is capable of analyzing a host of microstrip, stripline, or coplanar waveguide structures including discontinuities, transitions, spiral inductors, feed-thrus.

2. Microstripes. A suite of 3-D electromagnetic tools ideal for the design of waveguide components, non-planar circuit structures, transitions and a variety of antennas. It it based on the Transmission Line Matrix (TLM) method, which guarantees computation time and highly efficient use of memory. Typical applications include waveguide filters, couplers, waveguide to coax/microstrip transition, rectangular to circular guid transition, horn antennas, dielectric resonator filters, wire antennas, package effects. It calculates the impulse response of a device, filters the result, and resolve into incoming and outgoing waves before generating the scattering parameters.

3. Touchstone: A linear frequency-domain simulation design suite for microwave or RF circuit layouts.

4. PUFF: A scattering parameter and layout calculator for microwave circuits.

The commercial packaging units investigated were the LCC (0 - 23 GHz) package from StratEdge Corporation and the Dipak (0 - 40 GHz) from Dielectric Labs. Both are microstrip packages with the StratEdge package being leaded. These leads could be removed to facilitate direct connection to the microstrip. To access the non-idealities of these packages we must package a device with known electrical property. The device must mimic the input and output characteristics of the active device that we aim to package. Since our final goal is to package a MMIC amplifier, which has a 50 Ω input impedance and a 50 Ω output impedance, the simplest device will be a 50 Ω transmission line. The substrate that we use is 6-mil Arlon 350, with a relative dielectric constant of 3.5 $\pm$ 0.01. We fabricated a range of lines with different widths and lengths. We used the network analyser to find out the true impedances of each line, and the loss tangent of the substrate by comparing the loss of different line lengths.

To provide connections from the packages to the S-parameter measurement system two techniques were used. Firstly it was possible to wire bond CPW - microstrip launchers to the packages to enable measurements using a Cascade Probe station. Secondly the Wiltron Microstrip Universal Test Fixture (UTF) could on the StratEdge package for direct microstrip to microstrip connection.

Detailed results of these measurements and the models simulating their behavior are found in Ref [37] and the 1998 Annual Report. In summary, the fact that we can leave out width step and microstrip open end capacitance in Touchstone model without affecting the accuracy, while not so with the bond wires, illustrates that bond wires play a far more important role in microwave transitions, compared to height steps and width steps. and step in width. The number of bond wires affects the shape of frequency response while their lengths affect the magnitude. To have minimum insertion loss the bond wires should be as numerous and as short as possible.

With Touchstone we shall be able to predict circuit response for any chips with known S-parameters in these two packages. This will give us a fair indication of the circuit behavior without doing die attach for each chip, thereby reducing manufacturing cost and time.

SCIENTIFIC IMPACT

Several techniques of value in the generation of millimeter-wave modulated optical signals and in the characterization of lasers have been demonstrated.

The high-speed MSM detectors have been used in a novel optoelectronic circuit to phase-lock multiple lasers together in order to generate millimeter-wave beat signals. This approach has the potential to generate very high frequency signals. By using detectors fabricated on low-temperature grown GaAs for which bandwidths to 375 GHz have been demonstrated [2], it is conceivable that frequencies of many hundreds of GHz could be generated with a modest number of lasers.

The technique has been demonstrated with low-cost, commercially available laser diodes. Their ability to be used in an external cavity configuration suitable for an optical phase-locked loop has been demonstrated.

A new method for characterizing the FM response of lasers has been demonstrated. It relies on a self-heterodyne technique, and thus does not require stabilization of the absolute lasing frequency. It's simplicity and the fact that it uses the same experimental setup as the linewidth measurement are both attractive features. It could prove useful in the characterization of lasers used in coherent communication systems.

The packaging of microelectronic chips in many high speed/high frequency data processing/wireless communication units is the factor that determines or limits performance, cost and reliability. The work on packaging demonstrates that the effects of packaging can be evaluated and modeled, often with simple modeling tools, such as linear circuit simulators, up to frequencies as high as 40 GHz. The understanding gained can be used to design more efficient (lower loss, lower reflection coefficient) packaging interconnects.

REFERENCES

[1] F. Doany, D. Grischkowsky, and C. Chi, "Carrier Lifetime vs. Ion Implantation Dose in Silicon-on-Sapphire," *Applied Physics Letters*, 50, 460-462 (1987).

[2] Y. Chen, S. Williamson, T. Brock, F. Smith, and R. Calawa, "375-GHz-Bandwidth Photoconductive Detector," *Applied Physics Letters*, 59 (16), 1984-1986 (1984).

[3] E. Ozbay, K. Li, and D. Bloom, "2.0 ps, 150 GHz GaAs Monolithic Photodiode and All-Electronic Sampler," *IEEE Photonics Technology Letters*, 3, (6), 570-572 (June 1991).

[4] Y. Liu, W. Khalil, P. Fischer, S. Chou, T. Hsiang, S. Alexandrou, and R. Sobolewski, "Nanoscale Ultrafast Metal-Semiconductor-Metal Photo-detectors," *50th Annual Device Research Conference Digest*, VIB-1, (1992).

[5] A. Ketterson, J. Seo, M. Tong, K. Nummila, D. Ballegeer, S. Kang, K. Cheng, and I. Adesida, "A 10 GHz Bandwidth Pseudomorphic GaAs-GaInAs-AlGaAs MODFET-Based OEIC Receiver," *ibid*, VIB-5 (1992).

[6] D. Parker, P. Say, and A. Hansom, "110 GHz High Efficiency Photodiodes Fabricated from Indium Tin Oxide/GaAs," *Electronics Letters*, S66-67 (November 1989).

[7] J. Soole, H. Schumacher, H. Leblanc, R. Bhat, and M. Koza, "High Speed Performance of OMCVD Grown InAlAs/GaInAs MSM Photodetectors at 1.5 μm and 1.3 μm Wavelengths," *IEEE Photonics Technology Letters*, 1, (8), 250-252 (August 1989).

[8] C. Shi, D. Grutzmacher, M. Stollenwerk, Q. Wang, and K. Heime, "High-Performance Undoped InP/n-In0.53Ga0.47As MSM Photodetectors Grown by LP-MOVPE", *IEEE Transactions on Electron Devices*, 39, (5), 1028-1031 (1992).

[9] P. T. Chan, H. S. Choy, C. Shu and C. C. Hsu, "High-Performance Metal-Semiconductor-Metal Photodetectors with a Strained Al0.1In0.9P Barrier Enhancement Layer," *Applied Physics Letters*, 67, (12), 1715-1717 (1995).

[10] R. Yuang, H. Shieh, Y. Chien, Y. Chan, J. Chyi, W. Lin and Y. Tu, "High-Performance Large Area InGaAs MSM Photodetectors with a Pseudomorphic InGaP Cap Layer," *IEEE Photonics Technology Letters*, 7, (8), 914-916 (August 1995).

[11] T. Sugino, I. Yamamura, A. Furukawa, K. Matsuda and J. Shirafuji, "Improved Barrier Height of Phosphidized AlInAs," *Sixth IEEEConference on InP and Related Materials*, 632-635 (1994).

[12] I. K. Han, J. Her, Y. T. Byun, S. Lee, D. H. Woo, J. I. Lee, S. H. Kim, K. N. Kang and L. Park, "Low Dark Current and High-Speed Metal-Semiconductor-Metal Photodetector on Sulfur-Treated InP," *Jpn. J. Appl. Phys.*, 33, Pt. 1, No. 12A (1994).

[13] S. Gupta, J. F. Whitaker, S. L. Williamson, G. A. Mourou, L. Lester, K. C. Hwang, P. Ho, J. Mazurowski, and J. M. Ballingall, "High Speed Photodetector Applications of GaAas and $In_xGa_{1-x}As$/GaAs Grown by Low-Temperature Molecular Beam Epitaxy," *Journal of Electronic Materials*, 22, (12), 1449 (1993).

[14] J. Hugi, C. Dupuy, R. Sachot, and M. Ilegems, "Lifetime Limited Ultrafast Response of Metal-Semiconductor-Metal Photodetectors on GaInAs/GaAs-on-GaAs Superlattices," *Electronics Letters*, 29, (12), 1130 (1993).

[15] F. Hieronymi, D. Kuhl, E. H. Bottcher, E. Droge, T. Wolf, and D Bimberg, "High-Performance MSM Photodetectors on Semiinsulating InP:Fe/GaInAs:Fe/InP:Fe," *Fourth International Conference on InP and Related Materials*, 561 (1992).

[16] O. Wada, H. Nobuhara, H. Hamaguchi, T. Mikawa, A. Tackeuchi, and T. Fujii, "Very High Speed GaInAs Metal-Semiconductor-Metal Photodiode Incorporating an AlInAs/GaInAs Graded Superlattice," *Applied Physics Letters*, 54, (1), 16 (1989).

[17] R. Nagarajan, S. Levy, A. Mar and J. E. Bowers, "Resonantly Enhanced Semiconductor Lasers for Efficient Transmission of Millimeter Wave Modulated Light, " *Photon. Tech. Lett.*, 5, 4-6, (1993).

[18] J. B. Georges, M.-H. Kiang, K. Heppell, M. Sayed and K. Y. Lau, "Optical Transmision of Narrow-Band Millimeter-Wave Signals by Resonant Modulation of Monolithic Semiconductor Lasers," *Photon. Tech. Lett.*, 6, 568-570, (1994).

[19] C. R. Lima, D. Wake, and P. A. Davies, "Compact Optical Millimeter-Wave Source Using a Dual-Mode Semiconductor Laser," *Electronics Lett.*, 31, 364-366, (1995).

[20] A. C. Bordonalli, B. Cai, A. J. Seeds and P. J. Williams, "Generation of Microwave Signals by Active Mode Locking in a Gain Bandwidth Restricted Laser Structure," *Photon. Tech. Lett.*, 8, 151-153, (1996).

[21] K. J. Williams, L. Goldberg, R. D. Esman, M. Dagenais and J. F. Weller, "6-34\ts GHz Offset Phase-Locking of Nd:YAG 1319\ts nm Nonplanar Ring Lasers," *Electronics Lett.*, 25, 1242-1243, (1989).

[22] R. C. Steele, "Optical Phase-Locked Loop Using Semiconductor Laser Diodes," *Electronics Lett.*, 19, 69-70, (1983).

[23] J. Harrison and A. Mooradian, "Linewidth and Offset Frequency Locking of GaAlAs Lasers," *J. Quantum Electron.*, 25, 1152-1155, (1989).

[24] C.-H. Shin and M. Ohtsu, "Heterodyne Optical Phase-Locked Loop by Confocal Fabry-Perot Cavity Coupled AlGaAs Lasers," *Photon. Tech. Lett.*, 2, 297-300, (1990).

[25] H.R. Telle and H. Li, "Phase-locking of Laser Diodes," *Electronics Lett.*, 26, 858-859, (1990).

[26] J.M. Kahn, B.L. Kasper, and K.J.Pollock, "Optical Phaselock Receiver with Multigigahertz Signal Bandwidth," *Electronics Lett.*, 25, 626-628, (1989).

[27] R. T. Ramos and A. J. Seeds, "Fast Heterodyne Optical Phase Lock Loop Using Double Quantum Well Laser Diodes," *Electronics Lett.*, 28, 82-83, (1992).

[28] M. Kourogi, C.-H. Shin and M. Ohtsu, "A 134\ts MHz Bandwidth Homodyne Optical Phase-Locked Loop of Semiconductor Laser Diodes," *Photon. Tech. Lett.*, 3, 270-272, (1991).

[29] U. Gliese, T. N. Nielsen, M. Bruun, E. L. Christensen, K. E. Stubkjaer, S. Lindgren, and B. Broberg, "A Wideband Heterodyne Optical Phase-Locked Loop for Generation of 3-18 GHz Microwave Carriers," *Photon. Tech. Lett.*, 4, 936-938, (1992).

[30] O. Solgaard, J. Park, J. B. Georges, P. K. Pepeljugoski and K. Lau, "Millimeter Wave, Multigigahertz Optical Modulation by Feedforward Phase Noise Compensation of a Beat Note Generated by Photomixing of Two Laser Diodes," *Photon. Tech. Lett.*, 5, 574-577, (1993).

[31] K. Petermann, "Laser Diode Modulation and Noise." Dordrecht, The Netherlands: Kluwer Academic Publishers, (1991).

[32] E. Patzak, A. Sugimura, S. Saito, T. Mukai and H. Olesen, "Semiconductor Laser Linewidth in Optical Feedback Configurations," *Electronics Lett.*, 19, 1026-1027, (1983).

[33] R. Wyatt, "Spectral Linewidth of External Cavity Semiconductor Lasers with Strong Frequency Selective Feedback," *Electronics Lett.*, 21, 658-659, (1985).

[[34] T. Okoshi, K. Kkuchi and A. Nakayama, "Novel Method for Measurement of Laser Output Spectrum," *Electronics Lett.*, 16, 630-631, (1980).

[35] L. E. Richter, H. I. Mandelberg, M. S. Kruger and P. A. McGrath, "Linewidth Determination from Self-Heterodyne Measurements with Subcoherence Delay Times," *J. Quantum Electron.* 22, 2070-2074, (1986).

[36] D. Welford and S. B. Alexander, "Magnitude and Phase Characteristics in Directly Modulated GaAlAs Semiconductor Diode Lasers," *J. Lightwave Tech.*, 3, 1092-1099, (1985).

[37] K. E. Chiu, "*Microwave Packages Characterization and Simulation*", M.Eng. Thesis, School of Electrical Engineering, Cornell University, August 1998.

DEGREES AWARDED

Andrew Davidson, Ph.D, May 1997. "Generation and Detection of Millimeter-Wave Optical Signals for Use in Power-Combining Arrays."

Kaiwai Emily Chiu, Master of Engineering (Electrical), Cornell University, August 1998.

JSEP PUBLICATIONS

1. A. C. Davidson, F. W. Wise, and R. C. Compton, "High Performance MSM Photodetectors Using Schottky Contacts," *IEEE Photonics Technology Letters*, 5, 657-659, (1997).

2. A. C. Davidson, F. W. Wise, and R. C. Compton, "Low Phase Noise 33-40 GHz Signal Generation Using Multi-Laser Phase Locked Loops," *submitted to Photonics Technology Letters*.